Analysis of aroma-related volatile compounds affected by 'Ginsen Makuwa' genomic regions introgressed in 'Vedrantais' melon background

Perpiñá, G[1], Roselló, S[2], Esteras, C [1], Beltrán, J[3], Monforte, AJ[4], Cebolla-Cornejo, J[5], Picó, B[1]*.

[1] COMAV, Instituto de Conservación y Mejora de la Agrodiversidad, Universitat Politècnica de València, Cno. de Vera, s.n. 46022 València, Spain. E-mail: G.P.: gorperma@euita.upv.es; C.E.: criesgo@btc.upv.es; B.P: mpicosi@btc.upv.es

[2]Unidad Mixta de Investigación en Mejora de la Calidad Agroalimentaria UJI-UPV, Department de Ciències Agràries i del Medi Natural, Universitat Jaume I, Avda. Sos Baynat s/n, 12071 Castellón, Spain. E-mail: rosello@uji.es

[3]Instituto Universitario de Plaguicidas y Aguas (IUPA), Universitat Jaume I, Campus de Riu Sec, Avda. Sos Baynat s/n, 12071 Castellón, Spain. E-mail: beltranj@uji.es

[4]IBMCP, Instituto de Biología Molecular y Celular de Plantas (IBMCP) UPV-CSIC, Ciudad Politécnica de la Innovación Edificio 8E, Ingeniero Fausto Elio s/n, 46022 Valencia, Spain. E-mail: amonforte@ibmcp.upv.es

[5]Unidad Mixta de Investigación en Mejora de la Calidad Agroalimentaria UJI-UPV, COMAV, Universitat Politècnica de València, Cno. de Vera, s.n. 46022 València, Spain. E-mail: jaicecor@bct.upv.es

*** Corresponding author**

Tel:+34-963879415

E-mail: mpicosi@btc.upv.es

4.1. Abstract

Volatile organic compounds (VOCs) have an important role in melon flavour, one of the most important traits influencing consumer's preferences. The volatile profile of 25 introgression lines (ILs), developed from the Japanese cultivar 'Ginsen makuwa' (MAK) and the 'Charentais' cultivar 'Vedrantais' (VED), as donor and recurrent parent, respectively, was characterized in two environments. A total of 57 VOCs were identified using purge and trap extraction followed by chromatography-mass spectrometry. In addition, the IL population was genotyped with 2146 SNP distributed throughout the melon genome to tag Makuwa introgressions. The aromatic profiles of both parents (VED and MAK) and the hybrid revealed the genetic dominance of the MAK alleles against the VED alleles. MAK fruit displayed a significant decrease of most VOCs, mainly alkyl esters and apocarotenoid, compared to VED fruit, but had higher amounts

of some specific aldehydes, esters, and phenolic compounds, such aseugenol. MAK introgressions affected the production of VOCs in ILs. Although the environmental effect was remarkable, the trend of certain ILs was similar in both environments. Interesting ILs were detected with specific VOCs affected by specific MAK introgressions and also some ILs showed changes in VOCs profiles due to pleiotropic effects of changes in color flesh and the ripening process. Joint analysis of VOCs profile and ILs GBS genotypes allowed the identification of candidate genes for volatile production, such as MELO3C024886 (4-coumarate:CoA ligase) involved in the eugenol pathway, *CmCRTISO1* (MELO3C009571, carotenoid isomerase) related with the accumulation of carotenoids, precursors of the volatiles apocarotenoids, MELO3C006703 and MELO3C006545 (acyl-CoA ligases genes) involved in esters profile, and MELO3C030975 (aminotransferase) related with the aldehydes production. This study show how the use of genetic resources, such as those of the makuwa group, for breeding commercial melon can have an impact on the aromatic profiles.

Keywords: *Cucumis melo* L., introgression line, quality, genomics, metabolomics

4.2. Introduction

Melon (*Cucumis melo* L.) fruit quality is a complex trait which depends on many aspects such as fruit size, shape, color, texture, flavour and nutritional content. Flavour is one of the fruit traits that mostly determines the consumer perception of quality. It highly depends on the sweetness and acidity of the fruit flesh and on the fruit aroma profile. Aroma profile is characterized by a specific qualitative and quantitative pattern of volatile organic compounds (VOCs), especially abundant are esters, but also aldehydes, alcohols and terpenes, among others (Kourkoutas et al., 2006). Most of the VOCs affecting flavour increase at maturity and decrease when fruits are over-ripen (Beaulieu and Grimm, 2001). The final profile is the result of a combination of genotype and environmental effects (Bernillon et al., 2013). In adittion, the specific ability to accumulate precursors and/or to form and release conjugates during ripening are also important factors influencing the final profile (Rambla et al. 2016).

Melon is a highly polymorphic species (Pitrat, 2017), traditionally splitted into two subspecies subsp. *melo* and subsp. *agrestis*, and 19 groups. Accordingly, melon volatile profile is complex and more than 300 different compounds have been reported within the species, and more than 100 in a single cultivar (Gonda et al., 2016; Esteras et al., 2018).

Huge differences in the aroma profile between climacteric, more aromatic, and non-climacteric melons have been reported in several studies (Burger et al., 2006; Esteras et al., 2018). In climacteric melons, such as ‘Vedrantais’ (*C. melo* subsp. *melo* group Cantalupensis, subgroup ‘Charentais’), esters, low-odor threshold compounds with fruity, sweet, melon-like, and floral

aroma notes, are the main group of VOCs followed by alcohols and aldehydes, that also influence their unique aroma (Beaulieu and Grimm, 2001; Aubert and Bourger, 2004; Esteras et al., 2018). Non-climacteric melons, such as 'Piel de Sapo' melons (*C. melo* subsp. *melo* group Ibericus, sub-group 'Piel de Sapo'), however, present lower levels of esters and higher amounts of aldehydes and alcohols, displaying green, fresh, and cucumber-like aroma notes (Obando-Ulloa et al., 2010). A deep study of melon aroma using a large germplasm collection (Esteras et al., 2018) revealed more variability than expected within each melon group. In fact, four VOC profiles were reported within the Cantalupensis group, being the orange-fleshed 'Vedrantais' melons in the group with the highest levels of ethyl esters.

The group of Makuwa melons (*C. melo* subsp. *agrestis* group Makuwa) has an oriental origin and is extensively cultivated in the Far-East. These melons, which have dehiscent peduncles, have often been considered climacteric, but detailed characterization indicates an intermediate ripening behaviour between climacteric and non-climacteric melons (Leida et al., 2015). In fact, fruits drop from 'Vedrantais' plants when the fruit reaches the commercial ripening stage, while Makuwa fruits remain longer attached to the plant, even in more advanced stages of ripening. Makuwa melons have a thin and edible rind, white, sweet and crispy, juicy flesh, with an aromatic profile unique among the melons of the subsp. *agrestis*. According to their VOC profile, Makuwa melons clustered together with Near-East aromatic Dudaim melons (*C. melo* subsp. *melo* group Dudaim), close to aromatic cantaloupes (Esteras et al., 2018). This group of melons displays one of the highest total ester content among *agrestis* melons, being straight-chain esters (such as ethyl, butyl or hexyl acetate) especially important (Tang et al., 2015). Previous analysis report that Makuwa melons have approximately one third of the ester amount in 'Vedrantais' melons, with Makuwa having lower amounts of certain esters. The volatile profile of Makuwa fruit also varies during ripening (Li et al., 2016).

The genetic control of aroma production in melons has been studied in segregating populations derived from crosses between cultivars with contrasting VOC composition. Available genomic/transcriptomic tools have allowed the study of the genes involved in the aroma production (Freilich et al., 2015; Gonda et al., 2016; Gonda et al 2018; Tuan et al., 2019). Melon volatiles are mainly derived from fatty acids, aminoacids, and carotenoids. It is known that aldehydes, that contribute fresh and green notes to melon aroma, are produced from fatty acids *via* the action of lipoxygenases (LOX) and hydroperoxide lyases (HPL). Specifically, in the case of Makuwa melons it has been demonstrated that LOX enzymes play a central role in aroma production, promoting the accumulation of aldehydes and their derived esters (Tang et al., 2015). Aldehydes are also derived from aminoacids, such as L-phenylalanine, L-methionine and branched-chain aminoacids (L-leucine, L-isoleucine and L-valine), *via* aromatic and

branched chain aminoacid aminotransferases that generate the respective a-keto-acids (ArAT and BCAT), such as the encoded by genes *CmArAT1* and *CmBCAT1* characterized in melon (Gonda et al., 2016). Both fatty-acid and aminoacid-derived aldehydes contribute to fruit aroma, but are also precursors of alcohols and esters, the most important contributors to melon odor. Alcohols, the main constituents of non-climacteric melons aroma, are derived from aldehydes *via* alcohol dehydrogenases (ADH) such as the encoded by *CmADH1* and *CmADH2* (Manríquez et al., 2006), the two better charaterized genes in melon (Chen et al., 2016). Alcohols also serve as esters precursors through the esterification of an alcohol and acyl-coenzyme A (acyl-CoA) substrates by alcohol acyl-transferases (AAT). The acyl-CoA substrates are generated by acyl-CoA synthetases, also called acyl-CoA ligases, from fatty acids with varying chain lengths, short (acetic, propionic, butyric), medium (hexanoic, heptanoic, octanoid acids) and long-chain, that are used to form different esters. For example, the widely distributed acetate esters are formed with acetyl-CoA, while butyrate or hexanoate esters are derived from butyryl-CoA and hexanoyl-CoA, respectively. Different AAT enzymes use different substrates (alcohols/acyl-CoA) (Gonda et al., 2016). Several *CmAAT* have been functionally characterized (El-Sharkway et al., 2005) that differ in their substrate specificity. For example, *CmAAT1* is the most active producing a wide range of short and long-chain acyl esters and it has strong preference for the formation of E-2-hexenyl acetate and hexyl hexanoate, *CmAAT2* was thought to be inactive, but now is associated to the synthesis of several ethyl, thio and thioethyl esters, *CmAAT3* has a strong preference to produce benzyl acetate, and *CmAAT4* forms mainly cinnamyl acetate.

Some specific routes of volatile formation have been further studied, such as the biosynthesis of L-phenylalanine-derived volatiles, the most important compounds in melon aroma. These are produced by different biosynthetic routes. L-phenylalanine can be converted into phenylpyruvate by an aromatic aminoacid aminotransferase (*CmArAT1*) that later results into phenylacetaldehyde and phenethyl alcohol and its esters (Gonda et al., 2010). L-phenylalanine can also follow the phenylpropanoid pathway that involves the action of L-phenylalanine ammonia-lyase (PAL), generating (E)-cinnamic acid, a key intermediate. The gene *CmCNL* has been characterized which encodes for (E)-cinnamic acid:CoA ligase, that ligates (E)-cinnamic acid and CoA to form cinnamoyl-CoA, which is processed by cinnamoyl CoA reductase (CCR) to produce (E)-cinnamaldehyde (Gonda et al., 2018).

Oher VOCs, such as the phenylpropene eugenol, are also synthesized from L-phenylalanine *via* the phenylpropanoid pathway using (E)-cinnamic acid, followed by the action of (E)-cinnamic acid 4-hydroxylase (C4H) and p-coumaric acid CoA ligase (4CL) (Liu et al., 2018). Within the same route the melon gene *Cm*BAMT, encoding a benzoic acid:S-adenosyl-L-methionine

carboxyl methyltransferase, having a role in the accumulation of methyl benzoate from benzoic acid has been characterized.

The aminoacid L-methionine is also catabolized to produce sulfur volatiles *via* two different routes, one involving the conversion into the aldehyde 3-(methylthio)propanal by the L-methionine aminotransferase (MetAT), and the second involving the L- methionine- γ–lyase, ecoded by the gene *CmMGL* to generate methanethiol, further incorporated into sulphides and thioesters (Gonda et al., 2013; Gonda et al., 2016).

Other pathways to produce melon volatiles include the production of apocarotenoids *via* the oxidative cleavage of larger terpenoids, such as carotenoids, through the activity of carotenoid cleavage dioxygenases (CCD), such as the characterized *CmCCD1* (Ibdah et al., 2006; Vogel et al., 2008), and the production of mono and sesqui-terpenes from geranyl diphosphate (GPP) or farnesyl diphosphate (FPP) *via* terpene synthases (TPS) (Gonda et al., 2016).

The expression of many of the genes involved in the volatiles biosynthesis is regulated by ethylene changes, resulting in different volatile profiles in melons with different ripening patterns (Saladié et al., 2015).

Makuwa melons have gained attention as a possible source of interesting traits in melon breeding programs. Many disease resistances have been identified in this group (resistance to viruses, to Fusarium wilt and to *Aphis gossypii*) (Pitrat, 2017; Giner et al., 2017; Pascual et al., 2019) but they are also being used in breeding programs focused on melon quality. An introgression line (IL) collection has been recently developed by introgressing single fragments of the Makuwa genome (using the Japanese cultivar 'Ginsen makuwa' as donor parent) into the French cultivar 'Vedrantais' genetic background (Perpiñá et al., 2016). Some of these lines show features interesting for the diversification of the cantaloupe melons, such as variability in fruit traits (weight, fruit shape and flesh color), early maturing and delayed ripening, increased accumulation of metabolites (sugars and organic acids), etc. (Perpiñá et al., 2016, 2017), but it remains unknown how the Makuwa introgressions can influence the VOC profile of aromatic 'Charentais' melons.

In the present study, we analysed the VOC profile of this IL collection and used a genotyping by sequencing (GBS) strategy to characterize the genomic introgressions of each IL. These aromatic and molecular profiles will be valuable to improve our knowledge of the genetic control of aroma development in melon.

4.3. Material and Methods

4.3.1. Plant material.

The two melon cultivars, the Japanese accession 'Ginsen makuwa', PI 420176, (MAK) (*C. melo* subsp. *agrestis* group Makuwa, sub-group 'Yuki'), donor parent, and the cultivar 'Vedrantais' (VED) (*C. melo* subsp. *melo* group Cantalupensis, subgroup 'Charentais'), recurrent parent, were previously selected considering their contrasting phenotype regarding many traits, including a different fruit flesh VOC profile (Leida et al., 2015; Esteras et al., 2018). A set of twenty-five introgression lines (ILs) were developed by introgressing the genome of MAK in to the VED genetic background. MAK introgressions were defined with a set of 154 SNPs. The ILs showed an average of 1.3 introgressions/IL and covered nearly 100% of the donor genome (Perpiñá et al. 2016).

4.3.2. ILs Genotyping

In order to obtain a more accurate genomic characterization of Makuwa introgressions represented in the 25 IL set, this collection was further genotyped using the Genotyping-by-sequencing (GBS) strategy. DNA was extracted from three plants/IL with DNeasy Plant Mini Kit (Qiagen). GBS libraries were prepared using ApeKI and were subsequently sequenced using the HiSeq 2000 Illumina platform (Illumina Inc, San Diego, CA, USA) in the LGC Genomics GmbH (Germany) following the procedure reported by Elshire et al. (2011). Quality-filtered reads were mapped to the melon genome (assembly v.3.6.1; https://www.melonomics.net) using the GEM toolkit (version 3) (Marco-Sola et al., 2012). Alignment files containing only properly paired, uniquely mapping reads were processed using Picard (http://broadinstitute.github.io/picard/) to add read groups. The Genome Analysis Tool Kit (GATK) (McKenna et al., 2010) was used for local realignment. Variant calling was done using UnifiedGenotyper from GATK. Variants were filtered, the positions for which ones at least 1 sample had 10 reads were kept. Subsequently, the vcf file obtained was further filtered for MAF>0.01 and to avoid indels and excessive missing data (>10% missing data SNPs discarded).

4.3.3. Experimental design.

The same three plants per IL sampled for the GBS were grown under greenhouse conditions during the spring-summer season of 2015 in the Universitat Politècnica de València (UPV), in Valencia (39°29'00.4'N 0°20'28.0'W). Plants were transplanted the last week of March and fruits harvested during the second half of August. A replicate of this assay was conducted at the greenhouse facilities of the Fundación Cajamar in Paiporta (PAIP), in Valencia (39°25'05.8'N

0°25'03.4'W). Plants were transplanted at the beginning of March and fruits were harvested during the first half of July. In both locations, the three plants per IL were randomly distributed. Crop management and fruit harvesting at commercial maturity were performed as described by Perpiñá et al. (2016). Six plants of the recurrent parental (VED), the donor parent (MAK), and their corresponding F1 were also grown in PAIP as a reference.

4.3.4. Sample preparation and analysis conditions.

One fruit was harvested per plant, in both assays, PAIP and UPV, when the abscission layer appeared (commercial maturity for VED melons). In the case of lines MAK_7-2 and MAK10-1, that did not develop abscission layer (Perpiñá et al., 2017), fruit were collected at 45-50 days after pollination and checked for quality (appropriate flesh color, Brix degree, texture, and flavour). A cross-section of 10 cm was obtained from the equatorial plane of each fruit. Pericarp and approximately 2 mm of flesh, and seeds were discarded. The remaining flesh was homogenized (KRUPS KB720, Groupe Seb Iberica, Barcelona, Spain) and kept frozen at -80ºC until the analysis of volatile compounds. Three fruits per IL were sampled in each location, parentals were also sampled in PAIP assay, and equal volumes of the homogenate from the three fruits from each location were pooled for VOC analysis. Additionally, individual fruit samples of six fruits, three per location (PAIP and UPV), of each of 6 selected ILs (MAK_6-1, MAK_2-1, MAK_9-2, MAK_8-2, MAK_7-2, and MAK_4-1) were also analysed. These ILs were selected due to their specific phenotypes.

4.3.5. Reagents for metabolite analysis.

Reference standards of volatile compounds were supplied by Supelco (Sigma-Aldrich and Fluka; Barcelona, Spain) as pure compounds (90 - 99.5% purity) and individual stock standard solutions (500 mg L^{-1}) were prepared in acetone and used to generate mix standard solutions (using a 10-fold volume dilution steps). Calibration solutions were prepared from mix working solutions by consecutive volume dilutions with n-hexane to different final concentrations, according to the detector response for each compound. All standard solutions were stored at –18°C in sealed glass vials (avoiding any headspace). Gas chromatography grade solvents were obtained from Scharlab (Barcelona, Spain). Supelclean™ ENVI-Carb™ 120-400 mesh, 500 mg/6 mL SPE Tubes (Supelco, Barcelona, Spain) were used as traps.

4.3.6. Determination of volatiles.

Volatiles were extracted and determined following the methodology described by Fredes et al. (2016). The extraction was performed by dynamic headspace (DHS) using a purge & trap home-made device (Beltran et al., 2006; Sales et al., 2017) using commercial (500 mg) SPE cartridges as trap. Before analysis, trap cartridges were conditioned with 5 mL of diethyl ether (Et_2O), followed by 5 mL of n-hexane and finally vacuum dried for 10 minutes. A sample amount of 30 g of homogenized fruit was weighed into a 150 mL Erlenmeyer flask closed with a glass cap with two connection tubes; the inlet tube was connected to a dry nitrogen gas (N_2) source and the outlet tube to the trap. Extraction was performed at 40 ºC during 49 minutes with a nitrogen flow rate of 1.6 L min^{-1} and magnetic stirring at 300. Each trap cartridge was eluted after extraction with 5 mL of diethyl ether/hexane (1:1, v:v) followed by 5 mL of diethyl ether directly into a graduated glass tube. The extract was then evaporated under a gentle nitrogen stream at 35°C to a final volume of 0.5 mL. The final extract was divided into two aliquots and stored in a freezer at -20°C until their analysis by GC-MS.

A Varian CP-3800 gas chromatograph coupled to an ion trap mass spectrometry detector (Saturn 4000, Varian) was used for the determination of the volatiles. A 30 m×0.25 mm Supelcowax 10 (0.25 μm film thickness) capillary column was used for the separation, using helium at a constant flow of 1 mL min-1 as carrier gas. The temperature program was: 40°C for 5 min, then increased to 160 °C at 4 °C min^{-1}, and finally increased to 250 °C at 30°C min^{-1}, with a final isothermal stage of 1 min (total chromatographic analysis time 39 min). Injection of 1 μL of the sample in the splitless mode (injection port temperature 220°C) was performed using a Varian 8400 autosampler. MS (ion trap) measurements were performed in full scan mode (m/z scan range of 50 – 200 Da) using electron ionization (70 eV) in positive mode and external ionization configuration. GC-MS interface, ion trap, and manifold temperatures were set at 275°C, 190°C and 60°C, respectively.

For identification purposes, retention indices for all studied compounds were calculated by using a standard solution containing n-alkanes (C7-C30) and following the formula given by Kovats (1958). Quantitation was carried out by using external standard calibration curves using peak areas for the selected quantitation ion (Q) for each compound. Compounds with concentration exceeding linearity range were quantified by diluting extracts with n-hexane until proper concentration (Suppl. Table 1).

4.3.7. Data processing and statistical analysis.

Principal Component Analysis (PCA) with the volatile dataset was performed using S-Plus v. 8.01 for windows (Insightful Corp., Seattle). Hierarchical Cluster Analysis (HCA), using Euclidean distances and average linkage clustering, combined with heatmaps, using scaled data, were obtained with the online software *heatmapper* (http://www.heatmapper.ca). Correlation network analysis was conducted with the Expression Correlation (www.baderlab.org/Software/ExpressionCorrelation) plug-in implemented for the Cytoscape software (Shannon et al., 2003). Networks were visualized with the Cytoscape software, v3.3.0 (www.cytoscape.org). The nodes represented the volatiles groups (alcohols, aldehydes, esters, and apocarotenoids). Positive and negative correlations are indicated with black and red edges, respectively. Line thickness indicates correlation strength: the wider the line, the stronger correlation.

SNP calling results obtained from the GBS data were used to define the MAK introgressions of each IL. The physical position of flanking SNPs (located using the version CM6.3.1 (pseudomolecules) (https://www.melonomics.net) of the melon genome) with homozygous/heterozygous MAK/MAKVED genotypes defined each MAK homozygous/heterozygous introgression into the VED genetic background. Candidate genes reported previously to be involved in aroma-related VOC metabolism in melon (El-Sharkway et al., 2005; Galpaz et al., 2018; Gonda et al., 2010, 2013, 2018; Ibdah et al., 2006; Luccheta et al., 2007 Manriquez et al., 2006; Portnoy et al., 2008; Saladie et al., 2015; Tuan et al., 2019; Tzuri et al., 2015; Yahyaoui et al., 2002; Zhang et al., 2014) were located in these MAK introgressions, according to the melon genome annotation (CM 4.0 transcripts). Similar genes were found by mining the melon transcriptome using BLAST with the sequences of previously reported candidate genes and with the description of their functions as keywords. Qualitative or significant quantitative variation of specific VOCs were assigned to unique MAK introgressions of specific ILs, and the role of candidate genes located in the corresponding introgressions was discussed.

4.4. Results and discussion

4.4.1. GBS analysis of IL genotypes.

Approximately 143.000 SNPs with a minimum of 10 read depth were identified. They were subsequently filtered for mapping quality and to avoid excessive missing data, and finally, a set of 2.146 high quality SNPs, evenly distributed throughout the melon genome, were selected to better characterize MAK introgressions in each of these ILs.

The previous genotyping of this IL population with the Agena Bioscience genotyping (formerly Sequenom) platform (Perpiñá et al., 2016) detected 1.3 introgressions per line. With the new SNP set derived from the GBS the average increased to 2.77 introgressions per line (Fig. 1, Supp. Table 2). Most of the main introgressions previously detected were confirmed (average size 10.9 Mb), excep for MAK_9-1 that has no introgression in chromosome 9. Apart from the main introgression, this high density genotyping revealed additional introgressions with an average size of 1.7 Mb. Only 4.3 % of the MAK genome was not represented in the ILs collection. The gaps were located in chromosomes (Chr.) 1, 4, 5 and 7.

4.4.2. VOCs profiles of parents and ILs.

A total of 57 VOCs were identified in MAK, VED, F1 and the IL collection (Supp. Table 3). In the previous paper by Esteras et al. (2018), the profiles of VED and MAK were analysed. The total amount of volatile compounds in flesh tissue of MAK fruit was significantly lower than in VED fruit, with a reduction of 78% in total VOCs. This reduction was different among VOC groups, while total amount of alcohols, aldehydes, and acetate esters were only two to four times higher in VED than in MAK, the alkyl esters, the main contributors to the aroma of climacteric melons (Gonda et al., 2016), and the apocarotenoids volatiles, typical of carotenoid accumulating melons such as the orange flesh VED (Ibdah et al., 2006), were more than fifteen times higher in VED fruit compared with MAK. Our results confirm these differences and show a 66.2% reduction in total VOCs in MAK, being the highest reduction in alkyl esters and apocarotenoids amounts (Suppl. Table 3). Among the alkyl esters, the highest differences were found in the ethyl esters, ethyl butanoate, ethyl-2-methyl butyrate, and ethyl hexanoate that have been described as having an important role in the overall aroma profile of melon (Amaro et al., 2012; Beulieu and Grim, 2001; Gonda et al., 2016). The specific ester profile of MAK melons, rich in some straight-chain esters (such as butyl and hexyl acetates) (Suppl. Table 3) had been also reported in other works (Zhang et al., 2014; Tang et al., 2015; Li et al., 2016). Apart from the different ester and apocarotenoid profile, our assay show that MAK fruits had higher amounts than VED fruits of some compounds of the phenylpropanoid pathway, such as eugenol (Suppl. Table 3). Eugenol has been associated with the aroma of the Queen Anne's Pocket melon (*C. melo* group Dudaim) (Aubert and Pitrat, 2006), and higher contents of this compound in MAK compared to VED fruits were also reported by Esteras et al. (2018).

In general, the F1 (VED x MAK) fruit VOC profile was more similar to MAK than to VED (Suppl. Table 3), suggesting a dominant gene action of MAK over VED alleles. Also, most ILs showed lower amount of VOCs than VED, with an average reduction of 33.26% (from a 3.53% increase of MAK_9-1 to a 61.40% reduction of MAK_11-2). This decrease was variable among VOC groups. In order to better analyse the variability of VOCs profile in the experiment, a PCA and a heatmap with PAIP data for parents, F1 and ILs were performed (Fig. 2a and 3a). In the

PCA, the first two principal components explained the 20.07% and 14.39% of the variation respectively. The PCA confirmed a clearly different VOCs profile between both parents. The first component separated VED fruit from MAK, mainly due to its higher amounts of some alcohols (1-pentanol, (Z)-3-hexen-1-ol and 1-hexanol), and some aldehydes (hexanal, (E,E)-2,4-heptadienal, octanal and Z-6-nonenal), and due to its higher content of all apocarotenoids (6-methyl-5-hepten-2-one, genarylacetone, β-ionone, and β-ciclocytral) and specific abundant alkyl esters (mainly the aforementioned ethyl butanoate and ethyl-2-methyl butyrate) (Suppl. Table 4). As observed previously, the multivariate profile of the F1 was very similar to MAK. The heatmap shows the ILs more similar to both parentals (Fig. 3a). For example, the group of ILs with the highest content in alkyl esters (Suppl. Table 3), MAK_9-2, MAK_10-2, MAK_1-1 and MAK_2-1 were more similar to VED, except for their low content in apocarotenoids. MAK_6-1 was the most similar to MAK, with a similar quite low content in main alkyl esters, but a quite lower eugenol content, and MAK_3-1, MAK_4-2 and MAK_4-1 had also a more MAK-like profile.

4.4.3. Effect of the assay on VOCs content

The PCA performed with the ILs data of both environments (Fig. 2b) shows a higher variability in UPV than in PAIP environment. The effect of the assay on VOCs content was expected, as it is well known that volatiles are affected by environment (Beaulieu, 2006; Bernillon et al., 2013). In general, fruits of the ILs grown in PAIP had similar average alcohol levels than fruits harvested in UPV. Total alcohols averaged 936.92 *versus* 961.98 $ng.g^{-1}$ in PAIP and UPV (ranging from 498.74 to 2116.28 $ng.g^{-1}$ and from 218.95 to 2649.48 $ng.g^{-1}$, respectively) (Supp. Table 3). However, the total amount of aldehydes was higher in UPV (ranging from 13.95 to 230.73 $ng.g^{-1}$, with an average of 70 $ng.g^{-1}$) than in PAIP (15.36 to 90.23 $ng.g^{-1}$, with an average of 39.15 $ng.g^{-1}$). The two esters classes were differentially affected, whereas the amount of acetate esters was similar in both environments (970.79 $ng.g^{-1}$, range 206.44 to 1998.69 $ng.g^{-1}$ *versus* 862.52 $ng.g^{-1}$, range 241.45 to 1739.24 $ng.g^{-1}$, in PAIP and UPV, respectively), the total amount of alkyl esters was higher in PAIP (1523.73 $ng.g^{-1}$, ranging from 531.57 to 3202.29 $ng.g^{-1}$) than in UPV (1085.59 $ng.g^{-1}$, ranging from 223.48 to 3097.14 $ng.g^{-1}$). Regarding the apocarotenoids content, this was lower in PAIP (21.11 $ng.g^{-1}$, ranging from 2.72 to 84.44 $ng.g^{-1}$) than in UPV fruit (33.6 $ng.g^{-1}$, ranging from 1.23 to 59.72 $ng.g^{-1}$). Fruits were collected in both assays when the abscission layer appeared, but the different environmental conditions, among PAIP and UPV assays, might account for these differences. The aroma profile of UPV fruit suggests a delayed ripening in this environment.

The PCA indicated (Fig. 2b) that some ILs have similar profiles for the VOCs that explain most of the variation in both environments, but other show quite high environment effect. In general, MAK_2-3, MAK_3-1, MAK_5-2, MAK_7-2, MAK_8-1, MAK_10-2, MAK_10-3 and MAK_11_2 have similar profiles (all with high and significant correlations between environments, Suppl. Table 3), although with a higher ester content in PAIP samples in most cases. However, MAK_2-1, MAK_4-3, MAK_9-2, MAK_10-1 and MAK_12-2 have profiles in UPV and PAIP separated according to the first component (with UPV fruits richer in some specific acetate esters and alkyl esters, mainly butyrates, such as propyl butyrate and ethyl-2-methyl butyrate), whereas UPV and PAIP profiles of MAK_1-1, MAK_4-2, MAK_5-1, MAK_6-1 and MAK_11-1 are separated according to the second component (with UPV samples having higher levels of some aldehydes, hexanal or nonanal, and apocarotenoids, but lower of alkyl esters). The ILs MAK_2-2, MAK_4-1, MAK_6-2, MAK_7-1, MAK_8-2, MAK_9-1 and MAK_12-1 were separated according with both components and had the highest effect of the environment over the main VOCs profile.

The heatmap with the data of the PAIP (Fig 3 a) and VED (Fig 3 b) also show this environmental effect, although it reflects some similarities in both assays. ILs were grouped into two main clusters in both environments, one with a few ILs more similar to VED with high alcohol and alkyl esters content, although low in apocarotenoids (consistently MAK_2-1 and MAK_9-2), and the main one with most of the ILs more similar to MAK, subdivided in two main subclusters, onewith a more MAK-like profile (being consistently MAK_6.-1, MAK_4-1, MAK_4-2 and MAK_3-1), and the other with some ILs with consistent similar VOCs profiles in both environments (such as MAK_2-2 and MAK_7-1). Some lines maintained high levels of specific volatiles in both environments, such as the MAK_1-1, the one with the highest levels of eugenol and MAK_4-3, the one with the lowest reduction in apocarotenoid levels compared with VED and rich in aldehydes (Suppl. Table 3).

4.4.4. Correlation network among VOCs

Correlations of VOCs contents between both environments were calculated (Supp. Table 5). A 40% of VOCs showed moderate significant correlations (R^2>0.35). Interestingly, these significant correlations between both environments were found in some of the main alcohols and aldheydes (1-hexanol, hexanal, and phenylacetaldehyde) and also within the group of alkyl esters, which have deep effects on melon aroma perception, and also apocarotenoids. The lowest correlation occurs in the acetate esters. A Cytoscape analysis was run to study VOCs network interactions (Fig. 4). The network obtained mostly identified correlations within groups of compounds for esters, aldehydes, and apocarotenoids. In the case of esters, two sub-

groups were identified considering the correlations registered. The first group included acetate esters and the butyrate subgroup of alkyl esters, except from the ethyl-2-methyl butyrate. Compounds from this first group were found in similar concentrations in both parents or were more abundant in MAK than in VED melons as described above (Suppl. Table 3). The second group included other alkyl esters, more abundant in VED fruit, including ethyl-3-(methylthio) propanoate, ethyl butanoate, ethyl-2-methyl butyrate, and ethyl hexanoate, known to have a key role in setting the typical melon aroma profile (Beulieu and Grim, 2001; Amaro et al., 2012; Gonda et al., 2016). The highest within group correlations were found within these two esters groups, especially among some acetates, among butyrates, and among ethyl esters (penta, hexa and heptanoates). Freilich et al. (2015) and Esteras et al. (2018), employing a RIL population (derived from the cross between PI 414723 (*C. melo* group Momordica) and 'Dulce' cv. (*C. melo* group Cantalupensis), and a core collection of melon germplasm, respectively, found the highest correlations between acetate and ethyl esters, although all kind of esters were significantly correlated. Even using different materials, their clustering pattern in both studies was quite similar to the one obtained with these ILs.

Aldehydes grouped together, as previously reported by Esteras et al. (2018), with the exception of benzaldehyde, which appeared grouped with alcohols, and (E)-2-octenal which grouped with acetates. Within the group of aldehydes, higher correlations were found among C-9 aldehydes and phenylacetaldehyde.

Alcohols appeared mostly scattered among esters. Nevertheless, high correlations were found among C5, C6 and C8 alcohols. The fact that alcohols appeared scattered among esters was expected, as they are used as precursors by alcohol acyltransferases (AATs), in the formation of esters (Burger et al., 2006). Freilich et al. (2015) also found that ethyl esters grouped with their alcohol precursors.

Apocarotenoids strongly correlated among them and with the aldehyde (E,E)-2,4-heptadienal. The strong correlations among apocarotenoids was also expected. All of them derive from carotenoid degradation (Burger et al., 2006) *via* carotene cleavage dioxygenase (CCDs), as in the case of other vegetables such as tomato or watermelon (Ibdah et al., 2006; Lewinsohn et al., 2005). Following a similar pathway, the strong correlation between β-ciclo-cytral and β-ionone would point to the common origin from β-carotene degradation as reviewed by these authors. For the rest of apocarotenoids, geranylacetone would derive from carotenoids from the first half of the carotenoid biosynthesis pathway, as well as 6-methyl-5-hepten-2-one, which can also be derived from δ-carotene (Vogel et al., 2008).

4.4.5. Specific effects of MAK introgressions on VOC accumulation

High levels of eugenol in IL MAK_1-1

The IL MAK_1-1 was the line among the ILs with the highest levels of eugenol in both assays (4.92 and 1.94 $ng.g^{-1}$ in PAIP and UPV respectively). This phenylpropanoid was abundant in MAK and not detected in VED (Suppl. Table 3). The GBS data show that this line has a major introgression in Chr.1 (from 6.785.822 to 28.575.758 pb), that is only partially shared by MAK_6-1 (13.242.386 to 16.830.387 pb), and a small introgression in Chr. 7 (1.044.582 to 2.497.023 pb) that is shared with MAK_7-1, MAK_7-2 and MAK_10-1 (Suppl. Table 2). None of these ILs share this trait. Interestingly the specific region of MAK_1-1 contains one farnesyl pyrophosphate synthase *CmFPPS1* (MELO3C024967: 10.314.385-10.318.697 pb) (Suppl. Table 6), a key enzyme for the synthesis of terpenoids (Dubey et al., 2003; Saladié et al., 2105), and a 4-coumarate:CoA ligase (4CL) (MELO3C024886: 11.806.353-11.810.755 pb), involved in the synthesis of diverse compounds derived from the phenylpropanoid pathway. Specifically, 4CLs are involved in the conversion of hydroxycinnamic acids in their corresponding Coenzyme A esters, which are precursors in the synthesis of eugenol. In fact, the expression of 4CLs has been directly related with the production of eugenol in other species (Rastogi et al., 2013). MAK alleles of this gene present in MAK_1-1 could account for the high eugenol contents specific of this line.

In melon eugenol has been reported to be the major volatile constituent of the skin of 'Queen's Anne pocket melon' (*C. melo* group Dudaim) (Aubert and Pitrat 2006), a group of aromatic melons with a unique aroma, so it needs to be studied how this high eugenol level affects consumer perception of MAK_1-1 aroma. Additionally, increasing the knowledge on eugenol synthesis would have an added interest, as it has been related with antifungical and antimicrobial activity, and in tomato it has been show to contribute to defence against *TYLCV* (*Tomato yellow leaf curl virus*). Furthermore, eugenol has been described as a bioactive compound promoting benefits in human health, thus its accumulation would be interesting to increase the functional value of the fruit (Atkinson, 2016).

High levels of aldehydes and apocarotenoids in IL MAK_4-3

MAK_4-3 had a singular VOCs profile, with the highest levels of aldehydes recorded in both environments, including aldehydes with a high reported impact in green, leafy and fresh melon aroma, such as hexanal. At the same time, it was the IL with an apocarotenoid profile more similar to VED, contrasting with the profile of most ILs that reduced significantly the apocarotenoids content. The GBS analysis detected two introgressions in this IL, the one in Chr. 4 (33.060.774-34.122.550 pb) and an additional one in Chr. 11 (5.677.104-13.283.619 pb)

(Suppl. Table 2). This additional introgression is completely shared with MAK_4-2, another IL that do not display any of the two characteristic traits of MAK_4-3 aroma profile. Interestingly, the introgression in Chr. 4 of MAK_4-3 is only partially shared with MAK_4-1 (33.101.237-34.122.550 pb), an IL with moderate aldehydes and low apocarotenoids content. That is, MAK_4-3 has a specific introgression in Chr. 4 flanked by SNP_33.060.774 (MAKMAK genotype) and SNP_27.745.979 (VEDVED genotype), so genes within this region can not be discarded. This genomic interval includes two interesting genes involved in VOCs metabolism (Suppl. Table 6). One of them is MELO3C030975 (28.830.018-28.838.794 pb), a branched-chain-amino-acid aminotransferase. These type of enzymes are known to be involved in the synthesis of aldehydes from branched-chain aminoacids (Gonda et al., 2016). Thus, the presence of the MAK allele might be linked with the increase of aldehyde content detected in this line in comparison with VED. However, it would be necessary to increase the marker density in this interval to better define the recombination point, to see if the MAK allele of MELO3C030975 is introgressed or not. In this region also maps the carotenoid isomerase *CmCRTISO1* (MELO3C009571: 131.107.278- 31.114.107 pb; Saladié et al., 2015). *CmCRTISO1* isomerizes all four cis-double bonds in prolycopene yielding all-trans-lycopene from which different carotenoids are synthesized (Galpaz et al., 2013). The high apocarotenoids content found in MAK_4-3, unique among the ILs, could be related with specific carotenoids accumulation in this ILs associated to the function of the *CRTISO* MAK alleles in a VED genetic background. Further analyses of the MAK_4-3 carotenoid profile are necessary to test this hypothesis.

MAK VOCs profiles in MAK_6-1 and MAK_4-1

As stated before MAK_6-1 was the IL with the VOCs profile more similar to MAK. This IL had the highest number of MAK introgressions in the VED background (Suppl. Table 2) which probably account for this strong effect on VOCs. Its profile was studied in more detail by analyzing 6 individual fruits, three per enviroment (Fig. 5). The individual analysis confirmed the significant effect on the reduction of alkyl esters that most contribute to melon aroma (ethyl-3-(methylthio)propanoate, ethyl butanoate, ethyl-2methyl butyrate, ethyl pentanoate and ethyl hexanoate). However, MAK_6-1 had most acetate esters contents similar to VED. This low alkyl ester profile is shared with other ILs, such as the MAK_4-1 (Fig. 5), with which MAK_6-1 do not share genomic regions. MAK_6-1 has, however, an exclusive region in Chr. 6 (2.177.861-5.949.182 pb) (Suppl. Table 2) that includes the genes MELO3C006703 (5.190.527-5.193.590 pb; CoA ligase) and MELO3C006545 (4.040.429- 4.055.853 pb; long-chain acyl-CoA synthetase). Acyl-CoA synthetases, also called acyl-CoA ligases generate acyl-

CoA substrates from fatty acids that are used to form different esters by alcohol acyl-transferases (AAT) (Shalit et al., 2001; Gonda et al., 2016). In other crops, such as tomato, qualitative differences in ester composition have been related with differences in efficiency or acyl-CoA specificity of the AAT enzymes involved in ester synthesis (Goulet et al., 2015). Also in melon, Freilich et al. (2015) analysing a RIL collection showed that *CmAAT-1* (MELO3C024771: Chr. 11, 8.184.873-8.187.698 pb) produced eight out of ten prominent acetate esters, while *CmAAT-2* (MELO3C024766: Chr. 11, 8.060.892-8.063.565 pb) correlated with six compounds including ethyl esters, thio-esters, and thio ethyl esters (El-Sharkway et al., 2005; Lucchetta et al., 2007; Yahyaoui et al., 2002). MAK_6-1 has VED alleles of the two *CmAAT* genes, and also of two additional AAT genes, *CmAAT-3* (MELO3C024762 : Chr. 11, 7.933.534- 7.935.291 pb) and *CmAAT4* (MELO3C017688: Chr. 7, 26.408.004- 26.409.442). Differential production of acyl-CoA substrates by MAK alleles and differential AAT specificity of VED proteins may account for part of these differences in esters profiles. MAK alleles for *CmAAT* genes are in MAK_4-2, MAK_4-3, MAK_11-1, and MAK_11-2, ILs with MAK-like profiles that deserve further characterization.

The analysis of individual samples also confirms that MAK_4-1 showed important reductions in the content of alkyl esters (Fig. 5), while the levels of acetate esters were high. This profile is similar to that of MAK_6-1, but with higher content in some acetate esters (such as Z-3-hexen-1-ol, acetate) and in some alkyl ester (propyl butyrate). This IL presented three introgressions, two on Chr. 4 (1.743.247-2.994.383 pb and 33.101.237-34.122.550 pb) and one on Chr. 12 (14.951.154-22.514.823 pb) (Suppl. Table 2). Two genes located in the exclusive introgression of this IL on Chr. 4 are related to the production of aldehydes. MELO3C003373 (665.354-665.653 pb) is an allyl alcohol dehydrogenase, and MELO3C003454 (1.361.276-1.364.284 pb) is a branched-chain-amino-acid aminotransferase. MAK_4-1 also shares an introgression with MAK_4-2 and MAK_3-1, also with low levels of alkyls esters (Suppl. Table. 3), in which MELO3C003803 (4.801.220-4.803.110 pb), the *CmBAMT* gene maps, involved in the production of esters through the L-phenylalanine route. Further studies are needed to see if any of these genes affect alkyl content.

4.4.6. Pleiotropic effects of MAK introgressions

Some of the effects on volatile accumulation of MAK introgressions may have their origin in genes with pleiotropic effects affecting other traits, such as flesh color, color of the inner rind and ripening behaviour. In this sense, while most ILs showed the typical orange flesh with green inner rind of VED, MAK_2-1 and MAK_9-2 developed green fleshed fruits (Perpiñá et al., 2016). On the other hand, MAK_6-1, MAK_8-2, and MAK_12-1 presented a yellow band in

the internal rind, differing from the rest of ILs that had the typical VED, green, internal rind (described in Perpiñá et al., 2016). Other lines had altered ripening behaviour. It was the case of MAK_7-2 and MAK_10-1, which had already been described as non-climacteric in the previous study by Perpiñá et al., (2016). The VOCs profile of these lines was studied in more detail by analyzing individual fruit harvested in both environments and are further described below.

4.4.6.1. Green flesh and yellow inner rind

MAK_2-1 and MAK_9-2 presented the lowest apocarotenoids content (Fig. 5) compared with the orange-fleshed ILs. The major differences were found in the content of 6-methyl-5 hepten-2-one and mainly geranylacetone, much lower in these two ILs compared to VED and to the other ILs. This characteristic is likely due to the lack of carotenoid precursors, considering the green flesh of these lines. In fact, the low accumulation of these VOCs has been reported previously in melons with green or white flesh (Burger et al., 2006). Melon fruit flesh color can be white, green, and orange. The main carotenoid accumulated in orange-fleshed cultivars, such as VED, is β-carotene (Burger et al. 2009). Fruit flesh color is governed by two major *loci* in Chr 9 and 8. The gene underlying the *locus* of Chr 9 has been cloned and characterized, *CmOr* gene, MELO3C005449 (Tzuri et al. 2015). *CmOr* is involved in the regulation of chromoplasts, and their carotenoid storage capacities and formation (Tzuri et al., 2015). Two candidates have been proposed to explain the effect of the locus in Chr 8. One is *CmPPR1* (MELO3C003069), that encodes a member of the pentatricopeptide protein family, involved in processing of RNA in plastids, where carotenoid and chlorophyll pigments accumulate (Galpaz et al., 2018), and the second is MELO3C003097 (Protein SLOW GREEN 1, chlroplastic) (Zhao et al., 2019). Classic studies indicate that these *loci* interact epistatically: *CmO*r^{+}−/*Chr8*$^{+}$− and *CmOr*$^{+}$−/*Chr8Chr8* (allelic combinations have orange flesh, *CmOrCmOr*/Chr8^{+} − white flesh and *CmOrCmOr*/*Chr8Chr8* green flesh. MAK fruits are white-fleshed, so this cultivar has the recessive (no orange) allele *CmOr* and the white allele of the candidate of the *locus* in Chr8, *Chr8*$^{+}$, being the MAK genotype *CmOrCmOr*/*Chr8*$^{+}$*Chr8*$^{+}$. On the other hand, the VED cultivar has the dominant (orange) allele *CmOr*$^{+}$ and the recessive (green) allele of *Chr8* (whose presence is apparent in the green color of the inner rind of VED fruit), being the VED genotype *CmOr*$^{+}$*CmOr*$^{+}$/ *Chr8 Chr8*.

Both ILs MAK_2-1 and MAK_9-2 share a MAK introgression in Chr. 9 (21.547.871-25.241.434 pb), homozygous in both lines, that includes *CmOr* (MELO3C005449: 21.683.406–21.690.712 pb), and also share a VED genotype in the Chr. 8 region where map *CmPPR1* (MELO3C003069: 31.800.854- 31.807.421 pb and MELO3C003097: 32.003.211- 32.007.029

pb) (Suppl Table 2 and 6). Therefore, according to the GBS genotyping results, MAK_9-2 and MAK_2-1 would have the genotype *CmOrCmOr* (from MAK) and *Chr8Chr8* (from VED), displaying green flesh. The oxidative cleavage of carotenoids leads to the production of apocarotenoids and is catalyzed by a family of carotenoid cleavage dioxygenases (CCDs) (Gonda et al., 2016). CCDs often exhibit substrate promiscuity, which probably contributes to the diversity of apocarotenoids found in nature. We have found 6 CCD genes (Suppl. Table 6) in the melon genome, mapping at Chr. 1, 3 6 and 11, but no one is in MAK introgressions of MAK_2-1 and MAK_9-2, thus suggesting that the significant reduction in apocarotenoids is in these ILs a consequence of the lack of carotenoid precursors more than of the effect of CCD MAK allelles.

Regarding flesh color, a set of ILs showed a different phenotype. MAK_6-1, MAK_8-2 and MAK_12-1 have the inner rind yellow instead of green as VED and the other ILs (Perpiñá et al., 2016). The VOCs analysis in individual samples of MAK_6-1 and MAK_8-2 (Fig. 5) confirm a level of apocarotenoids significantly lower than that of VED, but higher than that of the green fleshed MAK_2-1 and MAK_9-2, mainly for 6-methyl-5-hepten-2-one and geranylacetone levels. MAK_6-1, MAK_8-2 and MAK_12-1 share an intogression including the MAK region in which map the two candidates of the *locus* in Chr8 involved with flesh color (white-green flesh) (MELO3C003069 and MELO3C003097). These ILs have the genotype $CmOR^{+}CmOR^{+}$ (from VED) and $Chr8^{+}Chr8^{+}$ (from MAK), that confers orange color to flesh, but the typical green color of the VED inner rind change to yellow color due to the dominant allele (white) of the *locus* in Chro8. This color change does not seem to differentially affect their apocarotenoid profile, as the two ILs with this phenotype analysed individually, MAK_6-1 and MAK_8-2, did not differ from ILs MAK_7-2 and MAK_4-1 (Fig. 5) that have the VED genotype for both *loci* $CmOr^{+}CmOr^{+}$*/Chr8Chr8* displaying fruit with VED-like flesh and inner rind color. The fact that ILs with VED genotype in *CmOr* and in *Chr8*, such as MAK_7-2 and MAK_4-1, have significantly lower amounts of apocarotenoids than VED parental suggest the influence of other genes on carotenoids precursors accumulation or cleavage to apocarotenoids in these and most ILs (Suppl. Table 3).

4.4.6.2. Climateric behaviour

MAK_7-2 and MAK_10-1 did not form an abscission layer at full maturity and exhibit a significant delay in the formation of the layer compared to VED (Perpiñá et al., 2016). Fruits from those ILs had also firmer flesh and higher sugar content than VED melons (Perpiñá et al., 2017). Interestingly, these two ILs share a common region in Chr. 10 (1.335.417-2.206.788 pb) where maps the gene MELO3C012215 (1.933.739-1.938.444 pb), a NAC domain-containing

protein that could be related with this trait, as recent research has associated another NAC domain transcription factor (MELO3C016540: Chr. 6, 27.663.292-27.665.351 pb) with melon climacteric ripening (Ríos et al., 2017).

Ripening behavior regulated by ethylene is related with the development of some VOCs, especially with those sensitive to ethylene production, such as esters and apocarotenoids (Freilich et al., 2015). In agreement, both lines showed low levels of esters and apocarotenoids compared to VED (Suppl. Table 3). The profile of MAK_7-2 was further studied with individual samples (Fig. 5). Its profile of alcohols was similar to VED, but with lower levels of some alcohols as 1-hexanol, one of the main alcohols of 'Charentais' melons (Beaulieu and Grimm, 2001; Allwood et al., 2014), and higher levels of (E,Z)-2,6-nonadien-1-ol (described as typical cucumber an melon odor) compared to VED and the ILs population. The aldehydes content was quite variable (Fig 5), but in general MAK_7-2 presented significantly lower values than VED of hexanal, and of other aldehydes more typical of cantaloupe melons, such as octanal (Obando-Ulloa et al., 2010; Bai et al., 2014). Interestingly, MAK_7-2 presented significantly higher values of benzaldehyde than VED and most ILs (Fig. 5). These changes in alcohols and aldehydes content can be a consequence of the delayed ripening, but also an effect of MAK introgressions with specific aminotransferases (Suppl. Table 2). Interestingly, in the specific region of Chr. 7 of MAK_7-2 (2.701.809-27.623.980 pb) maps MELO3C025614 (5.068.667-5.071.324 pb), the aromatic amino-acid aminotransferase *CmArAT1* (MELO3C025613: 5.071.692-5.075.274, Gonda et al., 2016), which catalyzes the conversion of L-phenylalanine to phenyl pyruvate from which benzaldehyde can be derived (Gonda et al., 2010). Also in this region map several MAK PAL genes (L-phenylalanine ammonia-lyase, MELO3C017809 (27.312.256-27.314.607 pb), MELO3C017810 (227.317.836-27.320.203 pb) and MELO3C017811 (227.322.473-27.324.829 pb), known to lead the L-phenylalanine through the phenylpropanoid pathway.

The low ester content of MAK_7-2 was confirmed (Fig. 5) as this IL displayed one of the lowest esters levels among the selected ILs (Fig. 5). It released levels of some specific acetate esters (amyl acetate, Z-3 hexen-1-ol acetate, hexyl acetate, heptyl acetate, and octyl acetate) and alkyl esters (Ethyl-3-(methylthio)propanoate, ethyl butanoate, ethyl-2-methyl butyrate, ethyl pentanoate and ethyl hexanoate) significantly lower, not only than VED, but also than other climacteric MAK-derived ILs. MAK_7-2 shows very low levels of the alkyl esters most relevant to the 'Charentais' aroma (Alwood et al., 2014; Spadafora et al., 2019) (ethyl butanoate: 402.1 *vs* 1452.2 $ng.g^{1}$; isobutyl butyrate: 0.31 *vs* 4.8 $ng.g^{1}$; ethyl hexanoate: 16.4 *vs* 450.65 $ng.g^{1}$, respectively for MAK_7-2 and VED), but also shows very low levels of acetate

esters that are typical of MAK melons (Bai et al., 2014), such as the hexyl acetate (11,7 *vs* 132,05 ng.g^{1}, respectively for MAK_7-2 and VED). The observed reduction of esters typical of both parents, VED and MAK, suggest pleiotropic effect of the ripening delay, although the effect of MAK alleles of genes directly involved in ester production located in MAK 7_2 specific introgressions could also account for part of these variations. For example, the alcohol acyl transferase *CmAAT4* (MELO3C017688: 26.408.004-26.409.442 pb) (El-Sharkawy et al., 2005; Lucchetta et al., 2007), involved in the formation of esters through the esterification of specific alcohols and acyl-coA, and demonstrated to be up-regulated during ripening and inhibited in antisense ACO, non-climacteric melons.

Despite the altered profile due to the ripening delay, the aroma of MAK_7_2 still differ from non-climacteric non aromatic melons, such as the non-climacteric model the Spanish cultivar 'Piel de Sapo' (*Cucumis melo* subsp. *melo* group Ibericus). The aroma of this melon has been studied in detail compared with that of the climacteric model VED (Obando et al., 2008; Esteras et al., 2018). 'Piel de Sapo' aroma has higher levels than VED of key aldehydes, such as hexanal, whose levels in MAK_7-2 were reduced compared to VED. Also the 'Piel de Sapo' profile is characterized by low acetate and alkyl esters, some of which are still similar to VED in MAK_7-2 (2-methyl propyl acetate, benzyl acetate and methyl-2-methyl butyrate).

Also the MAK_7-2 profile is richer in esters than that reported for VED melons in which climacteric ripening has been inhibited using the antisense gene aminocyclopropane-1-carboxylic acid oxidase (ACO), a key enzyme for climacteric ripening (Bauchot et al.,1998), as this non-climacteric VED melons reduce by a 97% the lower and potent odorants 2-methylpropyl acetate and ethyl-2-methylbutanoate, similar or only moderately reduced in MAK_7-2 compared to VED (2-methylpropyl acetate: 230.4 *vs* 144.8 ng.g^{1}; ethyl-2-methylbutanoate: 138,2 *vs* 927,85 ng.g^{1}). Also this non-climacteric line still retained levels of some of the main aroma contributors similar to those found in other climacteric ILs and VED. Then the intermediate climacteric ripening of MAK_7-2, along with the effect of MAK introgressions are not enough to completely block the ester profile.

MAK_7-2 also had a significant reductions of apocarotenoids content (Fig 5) similar to other ILs. This IL is orange fleshed and Perpiña et al. (2016) did not report flesh color differences with VED melons. In its specific introgression there are several genes involved in carotenoid biosynthesis, including *CmPSY3* (Chr. 7, MELO3C016185: 21.849.416- 21.852.838 pb; Saladié et al., 2015), MELO3C017709 (Chr. 7, 26.522.044-26.525.060 pb), a zeta carotene isomerase, a phytoene desaturase, *CmPDS* (Chr. 7, MELO3C017772: 27.001.123-2.7011.565 pb; Saladié et al., 2015), and MELO3C016224 (Chr. 7, 22.480.061-22.482.158 pb), a putative

epoxycarotenoid digoxygenase, related with the carotenoid degradation pathway). Further analysis are to see if carotenoid precursors are affected in this ILs that can affect apocarotenoids profile.

4.5. Conclusions

MAK introgressions in the VED background in general reduced the accumulation of VOCs in fruit. The F1 VOC profile suggest a dominant effect of MAK alleles. Our results showed a more pronounced reduction for alkyl esters and apocarotenoids than other VOCs families such as alcohols, aldehydes and acetate esters. Although a strong environmental effect has been observed between trials, we have found several ILs with similar profiles in both enviroments.

We detected interesting lines with specific VOCs affected by specific MAK introgressions with candidate genes. MAK_1-1 with the highest amounts of eugenol that contains a MAK 4CL gene (MELO3C024886, 4-coumarate:CoA ligase), which is involved in the eugenol pathway. MAK_4-3, with the highest level of aldehydes that has introgressed a MAK region with an AT gene (MELO3C030975, branched-chain-amino-acid aminotransferase) related with aldehydes production and *CmCRTISO1* (MELO3C009571, carotenoid isomerase) related with the specific carotenoids accumulation. MAK_6-1 with a VOCs profile similar to MAK, contains the acyl-CoA ligases MAK genes (MELO3C006703 and MELO3C006545) and alcohol acyl transferase VED genes *CmAAT-3* and *CmAAT-4*,that could explain the differences in esters profiles. Also, we observed some effects of the volatiles profiles that can be a pleiotropic effect of a differential carotenoids accumulation, such as the low levels of 6-methyl-5 hepten-2-one and mainly geranyl acetone in two green flesh IL (MAK_2-1 and MAK_9-2). Finally we reported the effect of an altered ripening pattern found in MAK_7-2 on esters and apocarotenoids profiles, resulting in a new ester profile different from classical non aromatic and non-climacteric inodorus melons, characterized by an intermediate accumulation of alkyl esters, the main contributors to melon aroma.

These results confirm the effect of different MAK introgressions on VED aroma. The information generated about the candidate regions and genes will be of interest to avoid negative effects when using MAK genetic resources in breeding programs and also to develop new lines with VED background but new aroma profiles.

Figure 1. Graphical representation of the genotype of 25 introgression lines obtained with the 2146 high quality SNPs identified from the GBS analysis. Blue colour represents the regions homozygous for the alleles of the recurrent parent ‘Vedrantais’, VED; Green colour represents regions homozygous for the alleles of the donor parent ‘Makuwa’, MAK; yellow colour represents regions heterozygous for MAK/VED alleles.

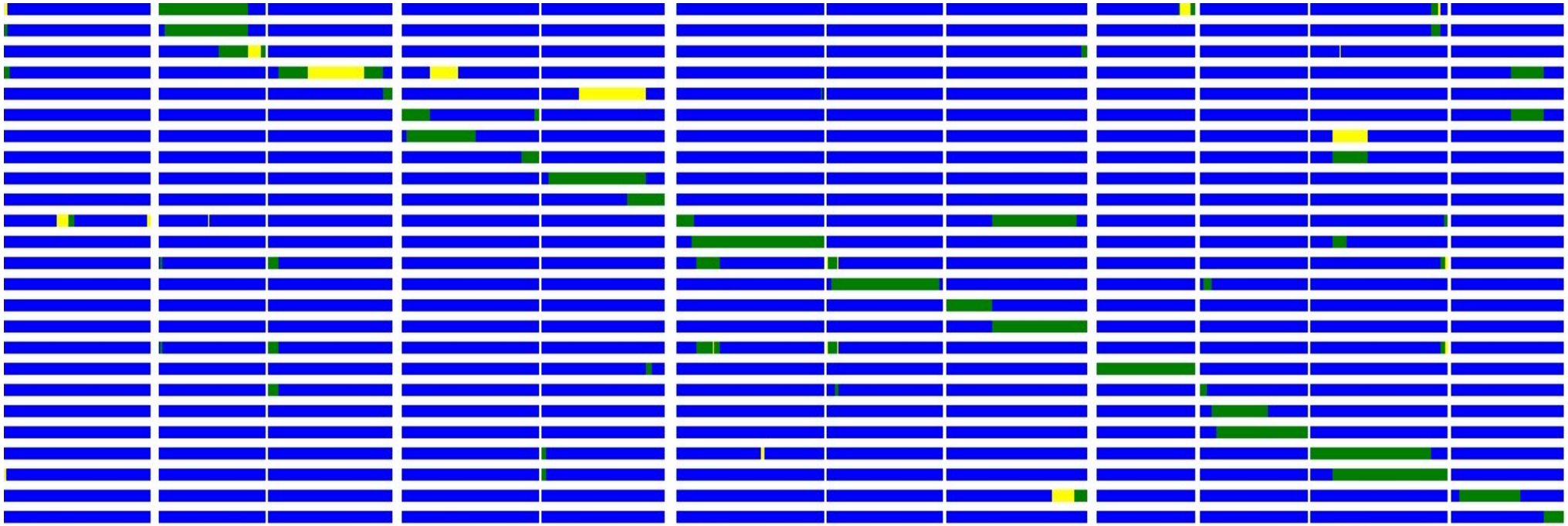

Figure 2. 2 a. Principal component analysis of the volatile data set. A) Loading plots of PC1 and PC2. Each volatile in the corresponding colour according to volatile groups (coded as in Supp. Table 1). B) Principal component analysis of the IL population, VED, MAK and F1 harvested in PAIP environment. C) Eigenvalue, percent of variance and cumulative percentage of PC1, PC2 and PC3. **2 b.** Principal component analysis of the volatile data set. A) Loading plots of PC1 and PC2. Each volatile in the corresponding color according to volatile groups (coded as in Supp. Table 1). B) Principal component analysis of the IL population in PAIP and UPV environment. C) Eigenvalue, percent of variance and cumulative percentage of PC1, PC2 and PC3.

.

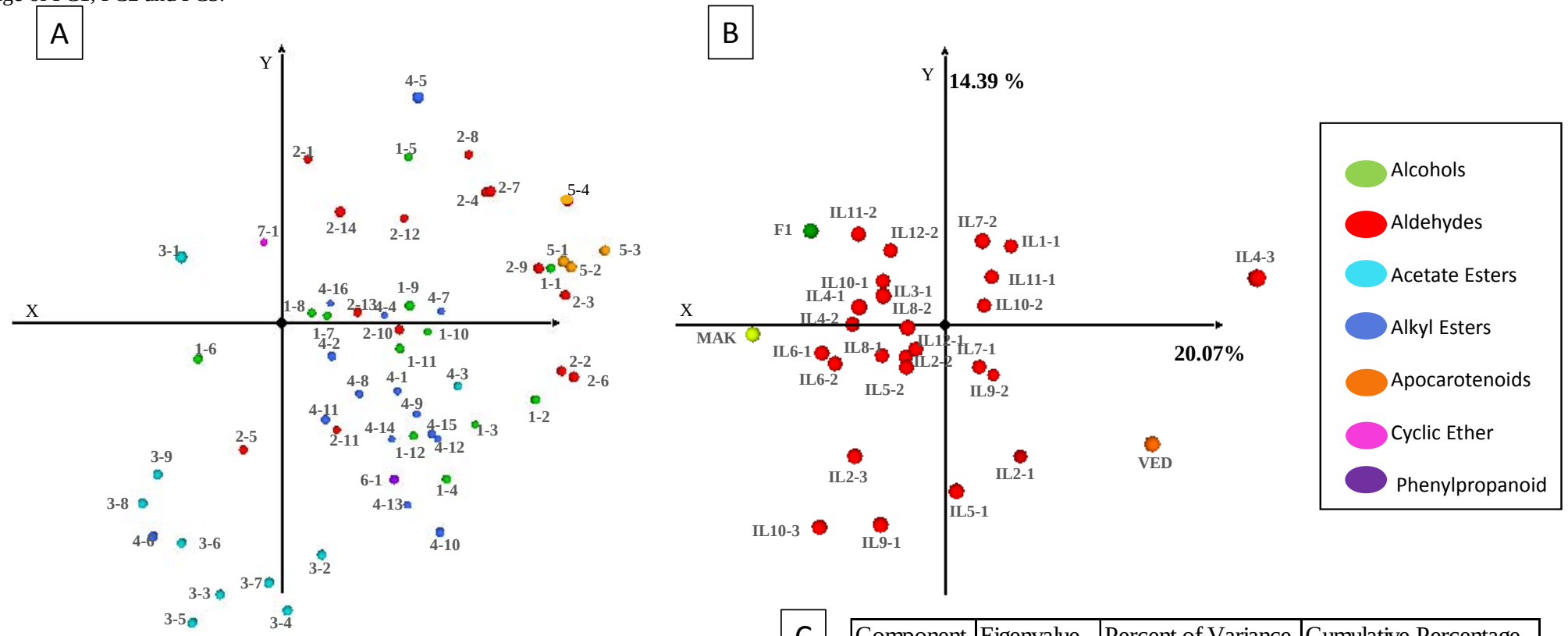

C

Component	Eigenvalue	Percent of Variance	Cumulative Percentage
1	11.43	20.07	20.07
2	8.20	14.39	34.46
3	6.30	11.05	45.51

Figure 3. 3a. Heatmap and cluster analysis (Euclidean distance, UPGMA) of the ILs lines grown in Paiporta, PAIP . Greenish colors imply higher contents of the volatiles, whilst reddish colors imply lower contents. Equivalence of figure codes of volatiles in Supp. Table 1. **3b.** Heatmap and cluster analysis (Euclidean distance, UPGMA) of the ILs lines Universidad Politécnica de Valencia (UPV) . Greenish colors imply higher contents of the volatiles, whilst reddish colors imply lower contents. Equivalence of figure codes of volatiles in Supp. Table 1

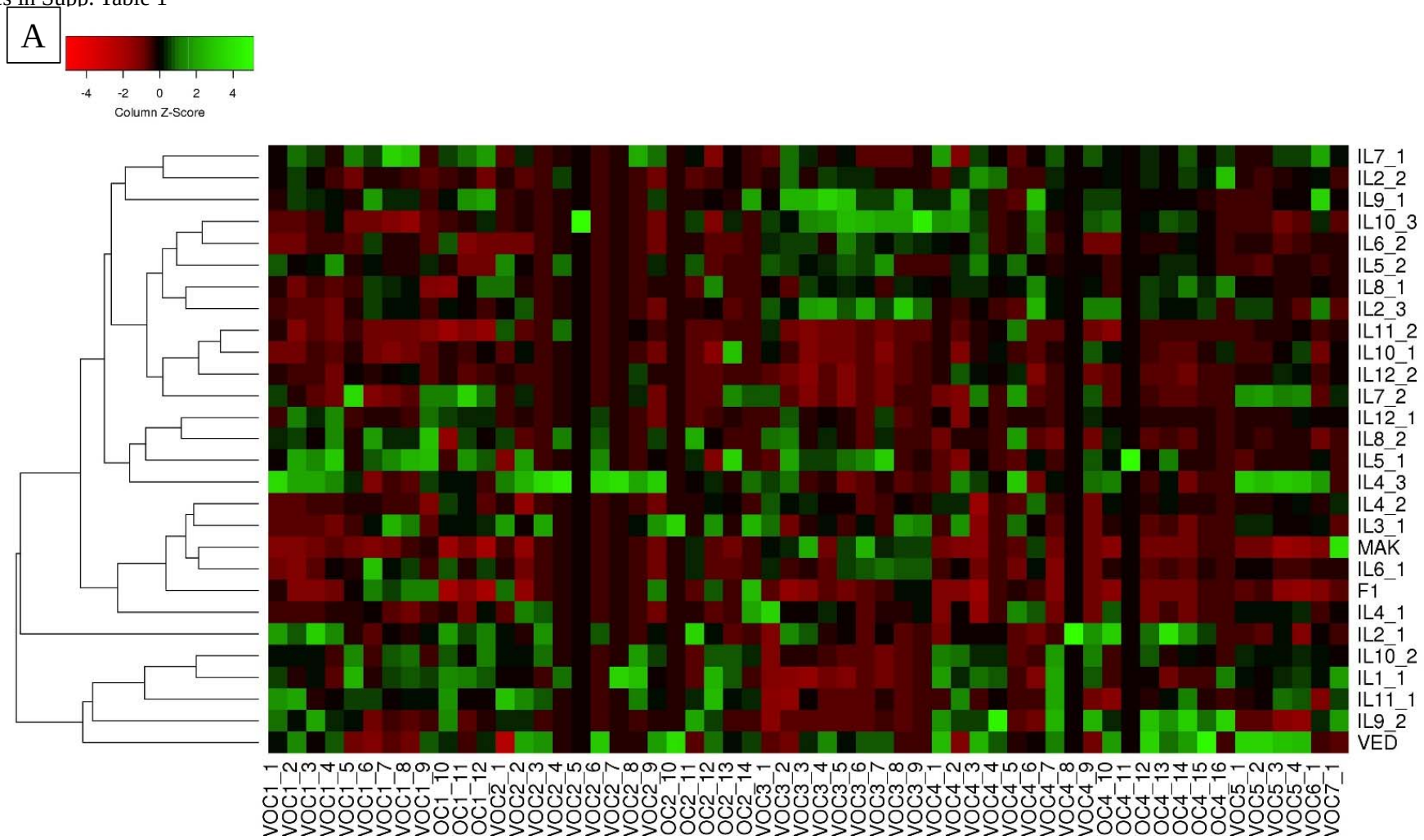

Figure 4. Correlation network analysis of the accumulation of volatiles. The nodes represent the volatiles, grouped considering their chemical family (see colour legend). Positive and negative correlations are indicated with black and red lines, respectively, with variable thickness considering their strength (see legend).

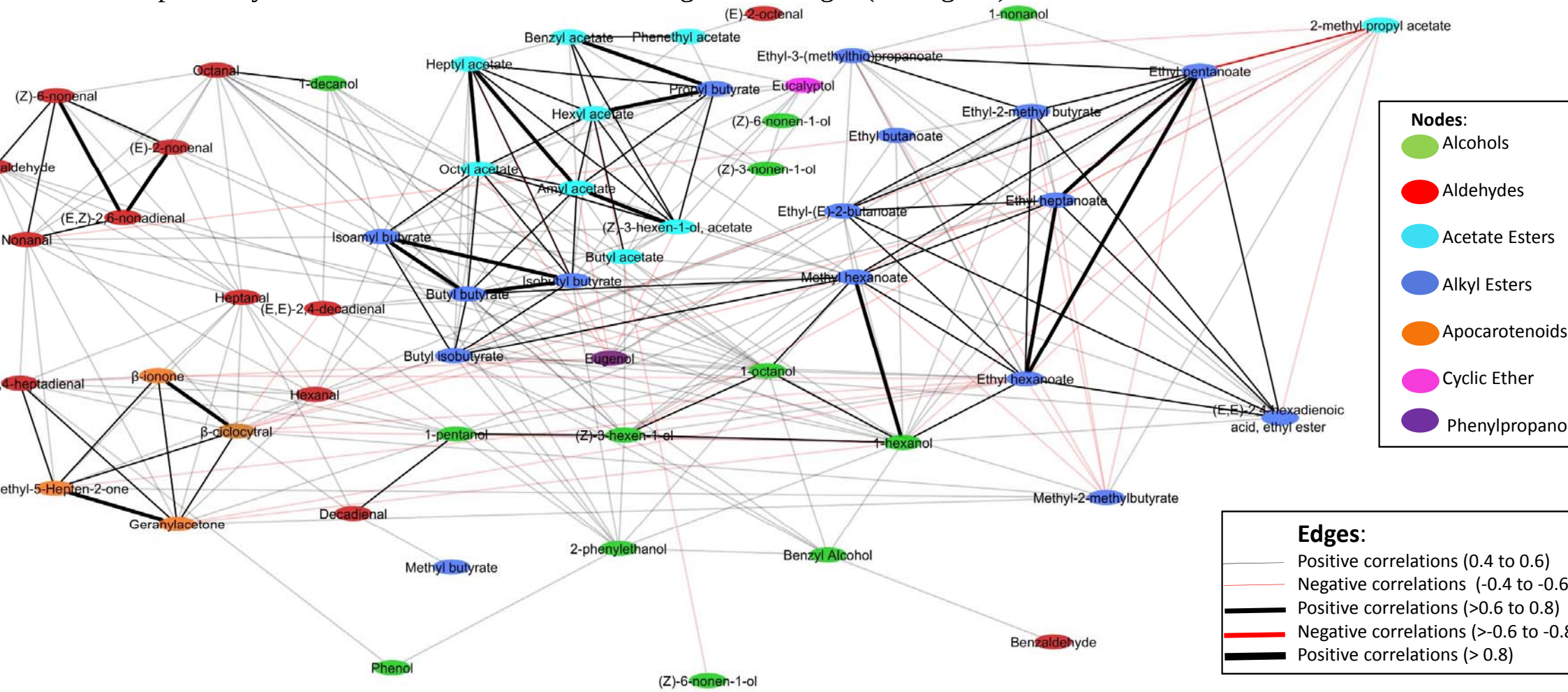

Quantities ($ng.g^{-1}$) of the compounds detected in the selected lines, for alcohols (Figure 5A), aldehydes (Figure 5B), acetate esters (Figure 5C), alkyl esters (Figure 5D), apocarotenoids, cyclic ether y penylpropanoid (Figure 5E). * Significant differences regarding VED in PAIP environment. Equivalence of figure codes of volatiles in Supp. Table 1.

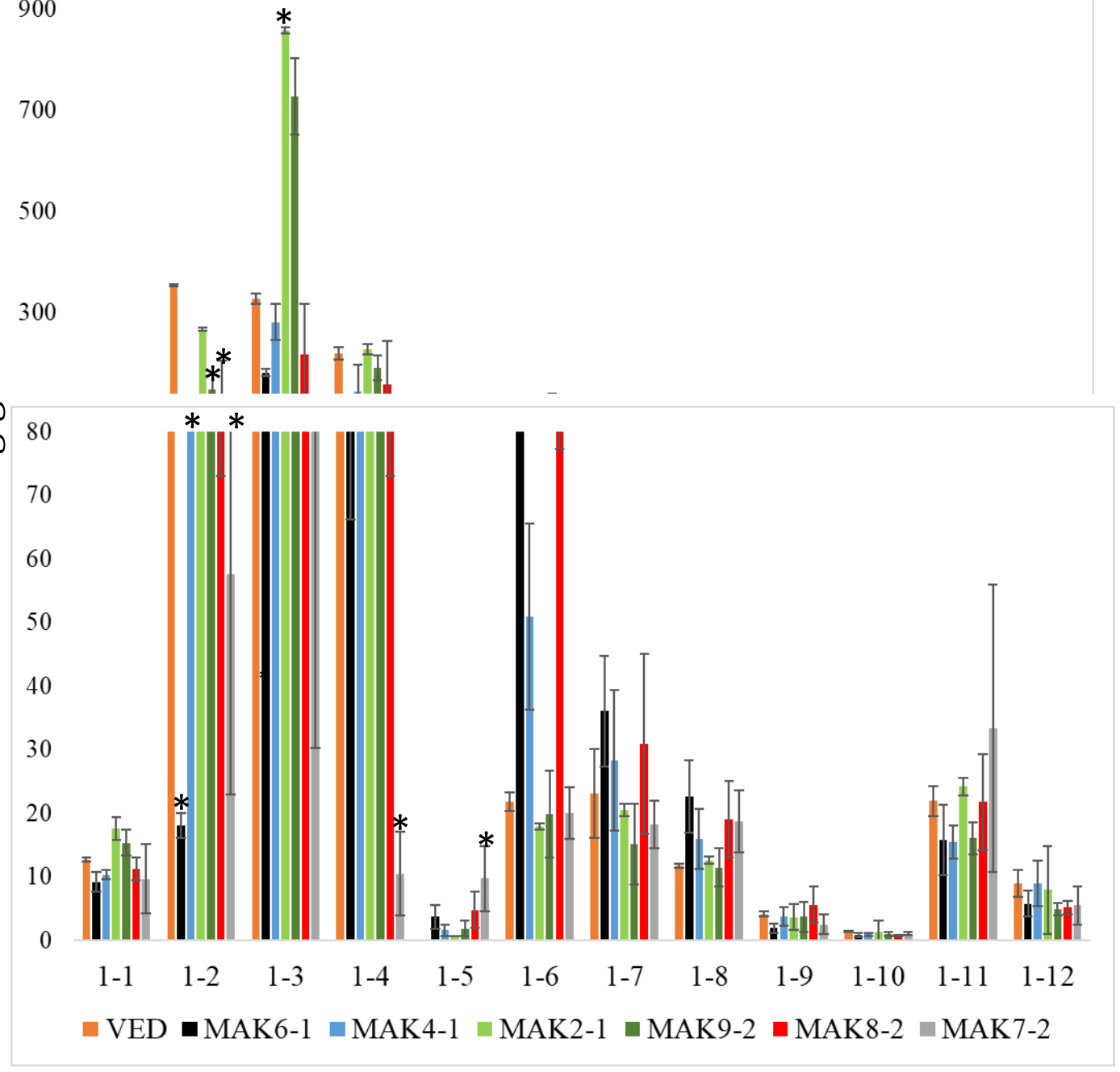
900
700
500
300
80
70
60
50
40
30
20
10
0
1-1
1-2
1-3
1-4
1-5
1-6
1-7
1-8
1-9
1-10
1-11
1-12
VED
MAK6-1
MAK4-1
MAK2-1
MAK9-2
MAK8-2
MAK7-2

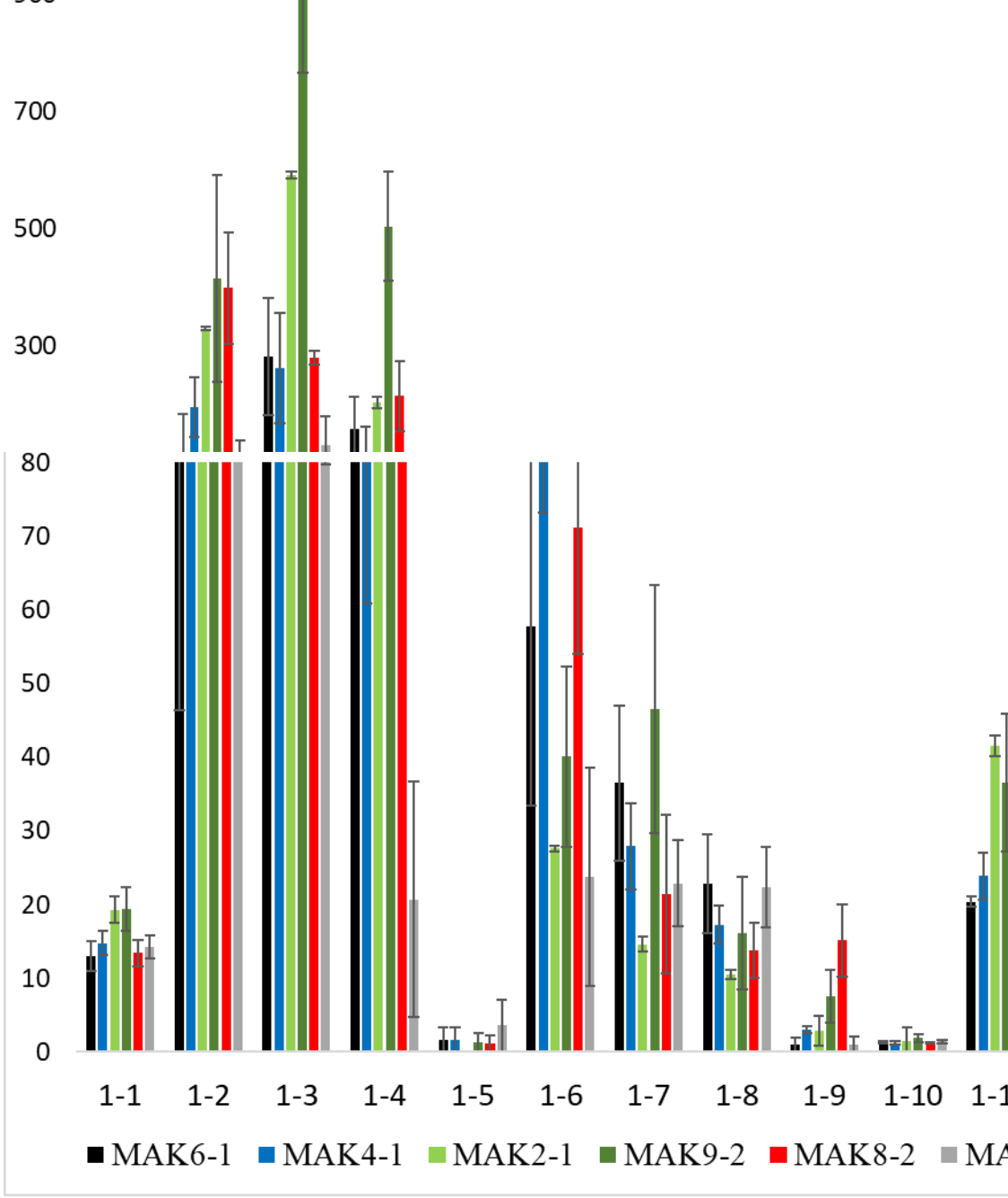
700
500
300
80
70
60
50
40
30
20
10
0
1-1
1-2
1-3
1-4
1-5
1-6
1-7
1-8
1-9
1-10
MAK6-1
MAK4-1
MAK2-1
MAK9-2
MAK8-2

B

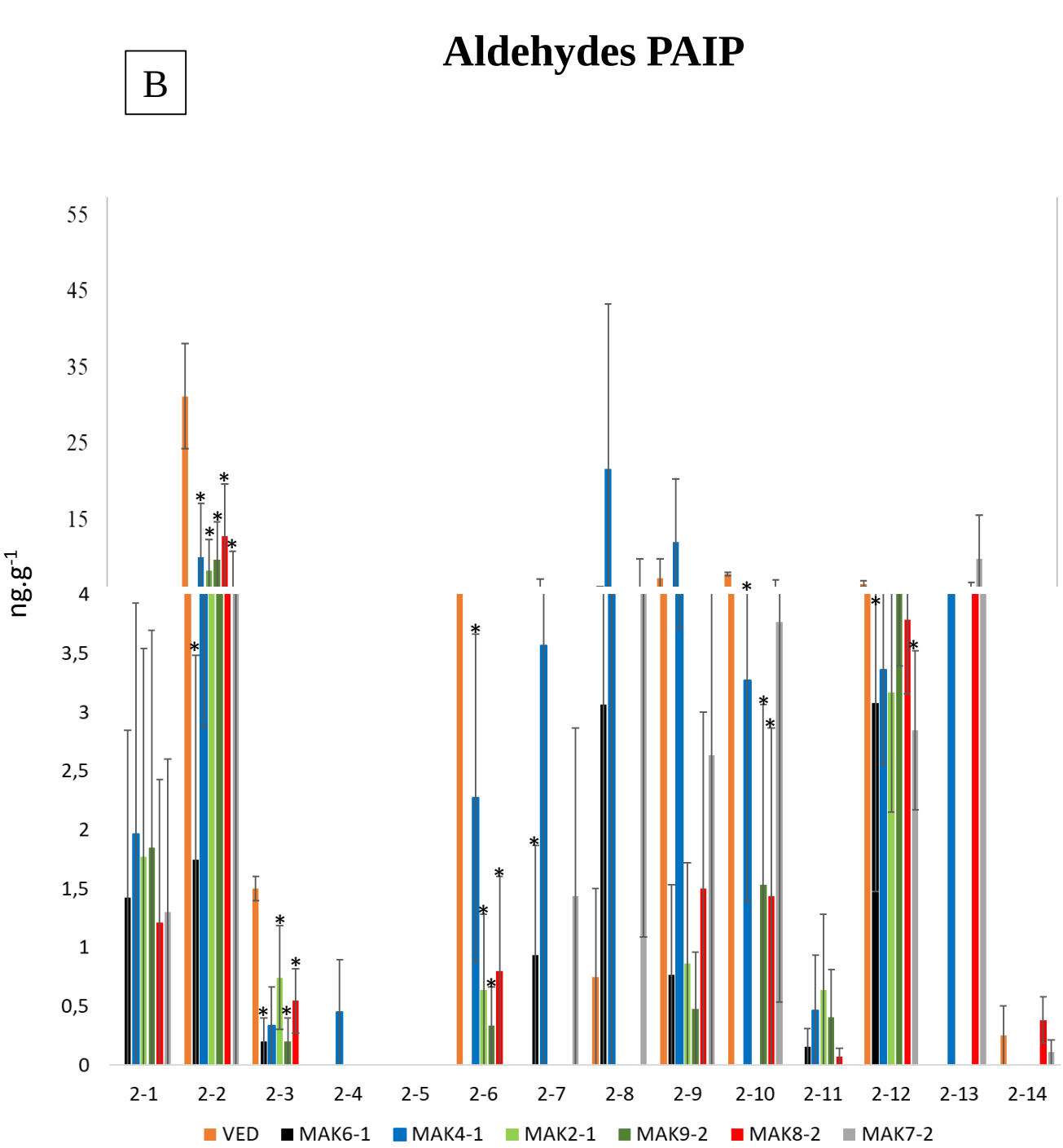
Aldehydes PAIP
ng.g-1
55
45
35
25
15
4
3,5
3
2,5
2
1,5
1
0,5
0
2-1
2-2
2-3
2-4
2-5
2-6
2-7
2-8
2-9
2-10
2-11
2-12
2-13
2-14
VED
MAK6-1
MAK4-1
MAK2-1
MAK9-2
MAK8-2
MAK7-2

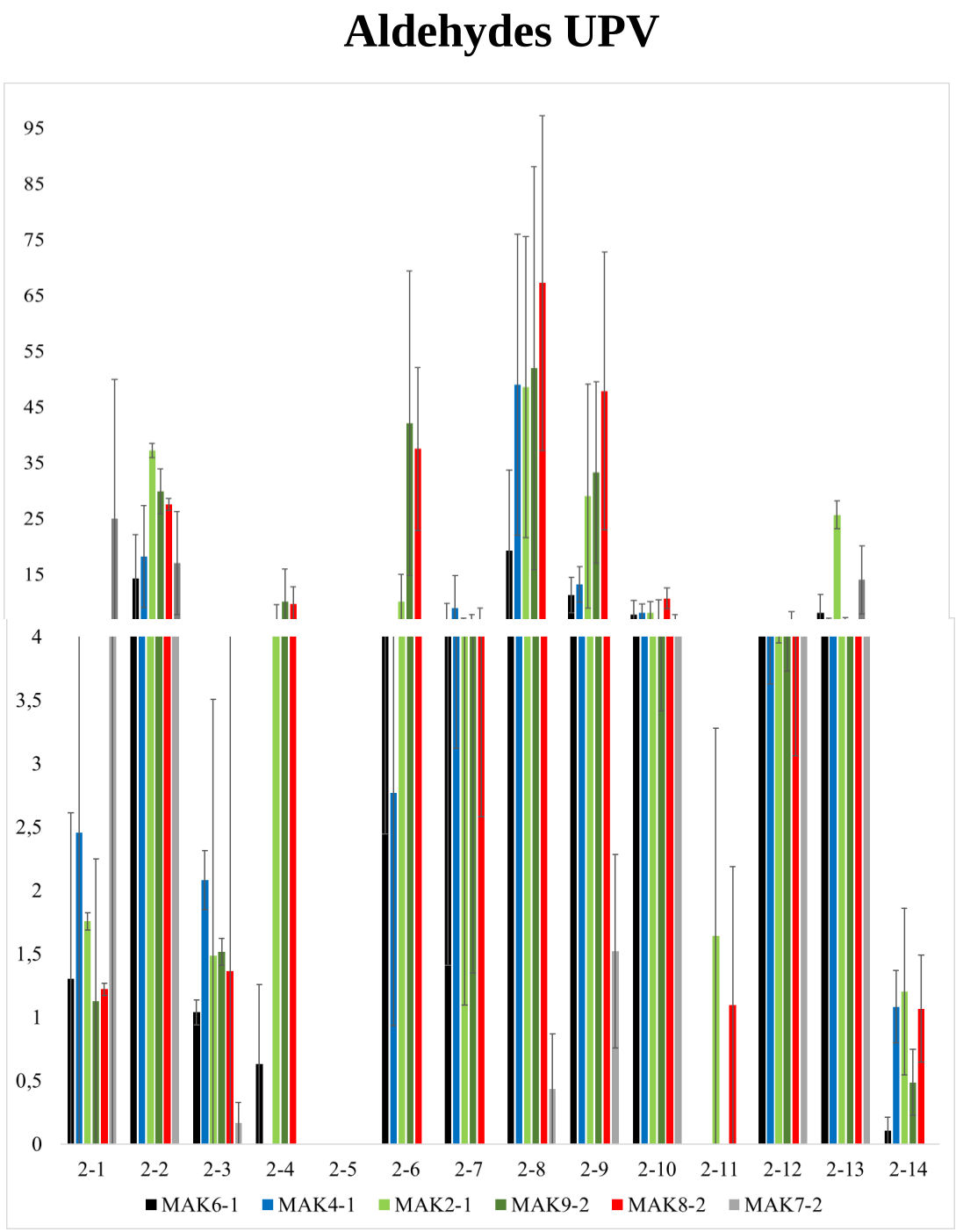
Aldehydes UPV
95
85
75
65
55
45
35
25
15
4
3,5
3
2,5
2
1,5
1
0,5
0
2-1
2-2
2-3
2-4
2-5
2-6
2-7
2-8
2-9
2-10
2-11
2-12
2-13
2-14
MAK6-1
MAK4-1
MAK2-1
MAK9-2
MAK8-2
MAK7-2

Acetate esters PAIP

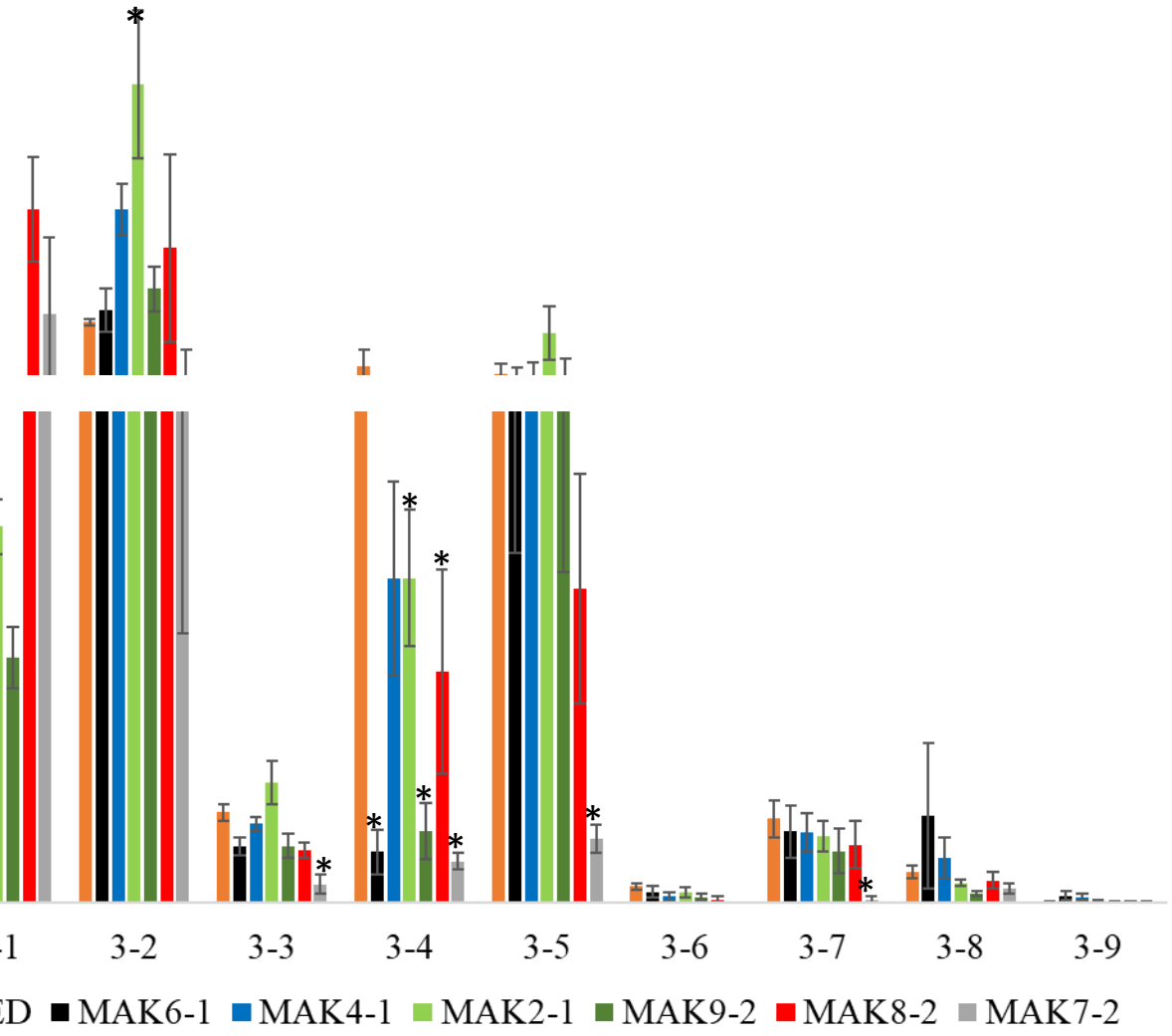

Acetate esters UPV

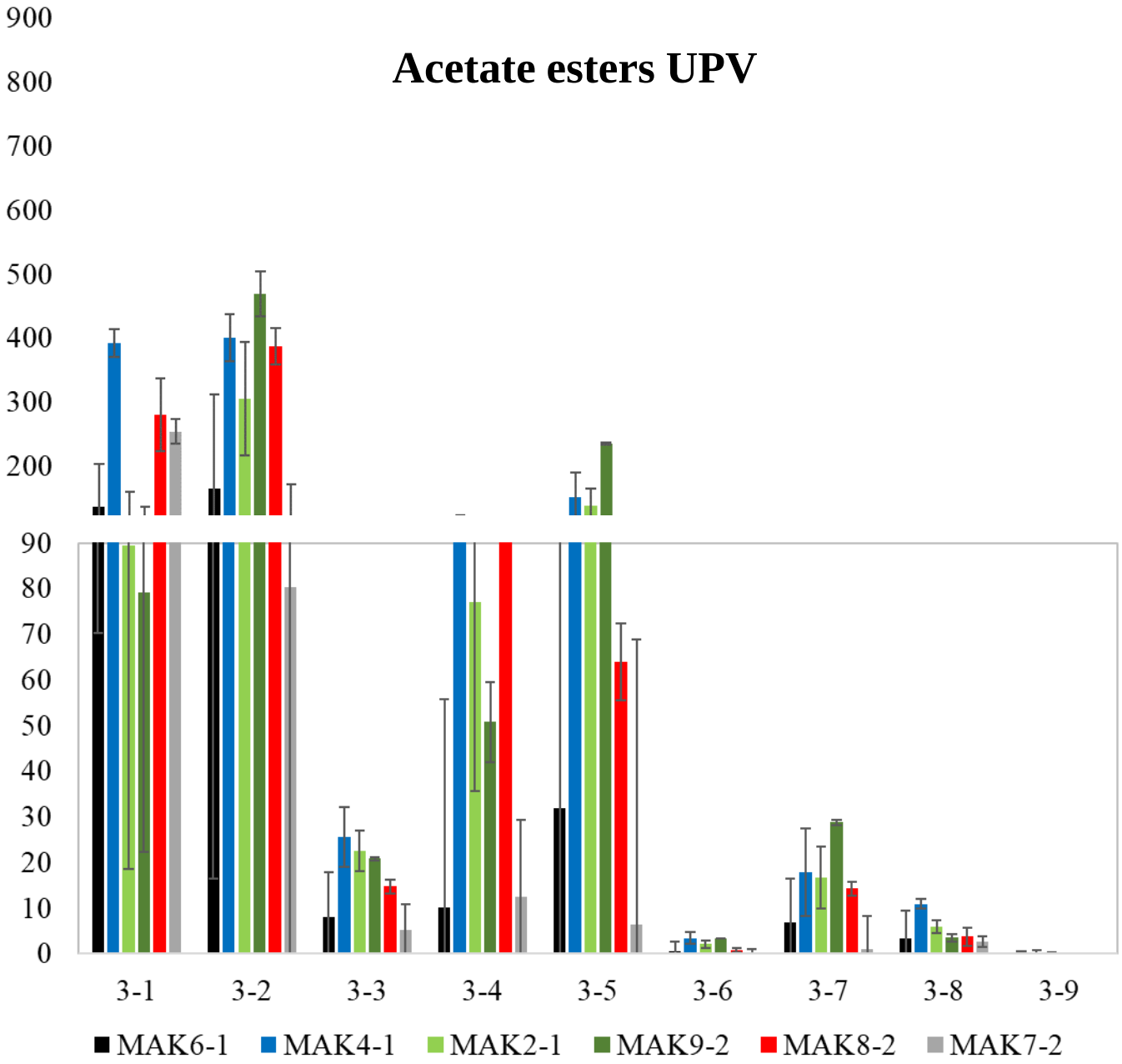

D

Alkyl esters PAIP

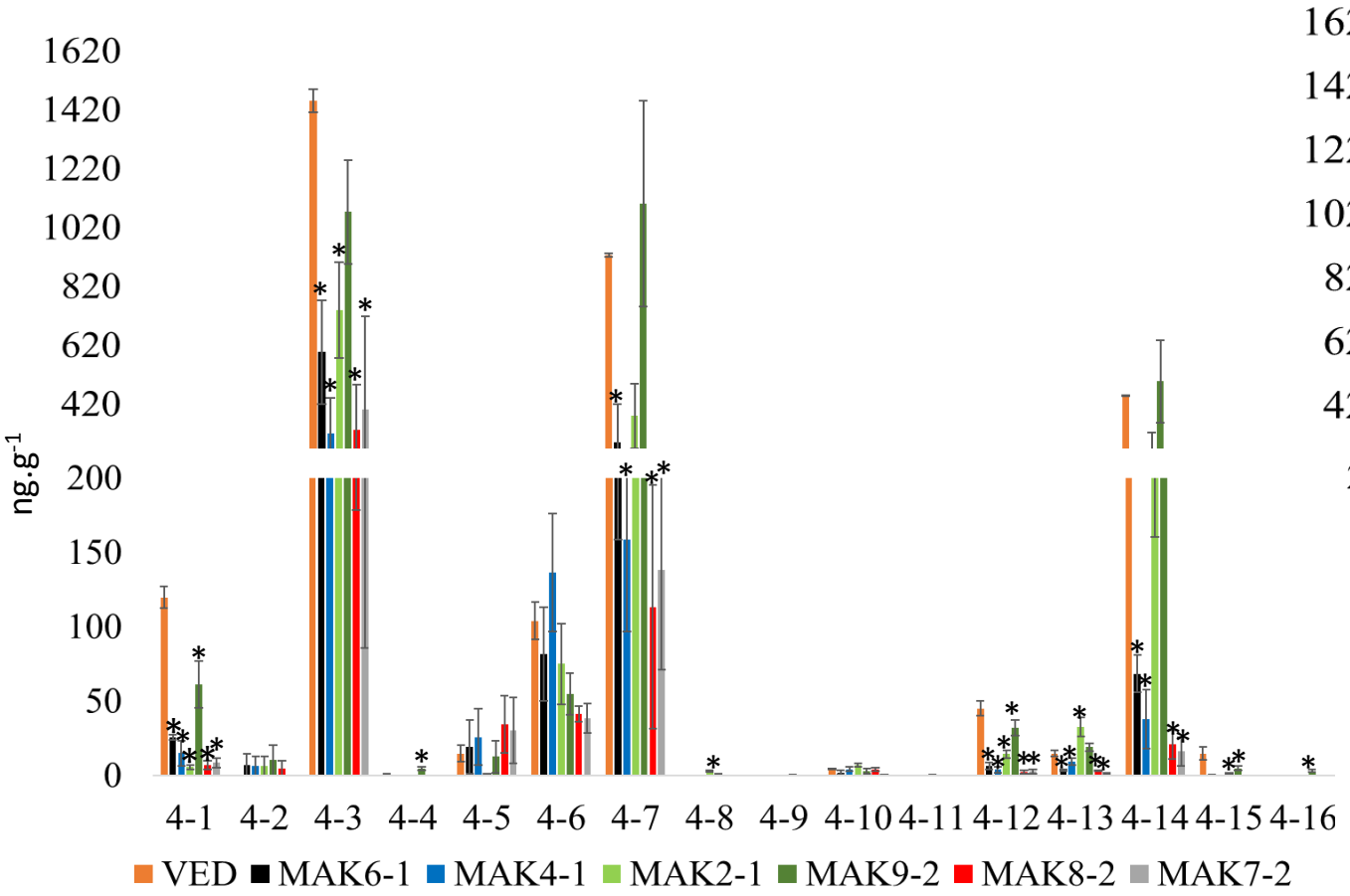

Alkyl esters UPV

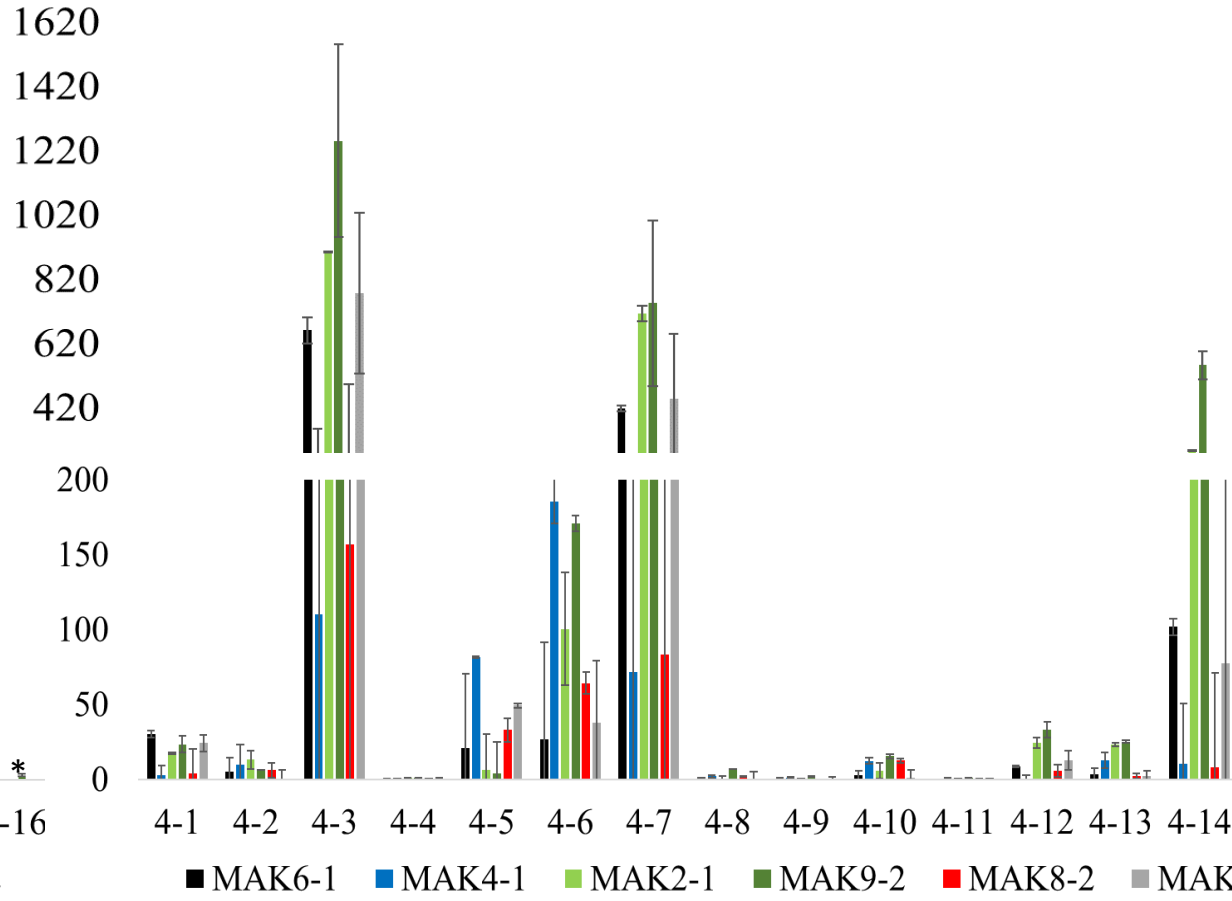

Apocarotenoids, Cyclic ether, Phenyl propanpid PAIP

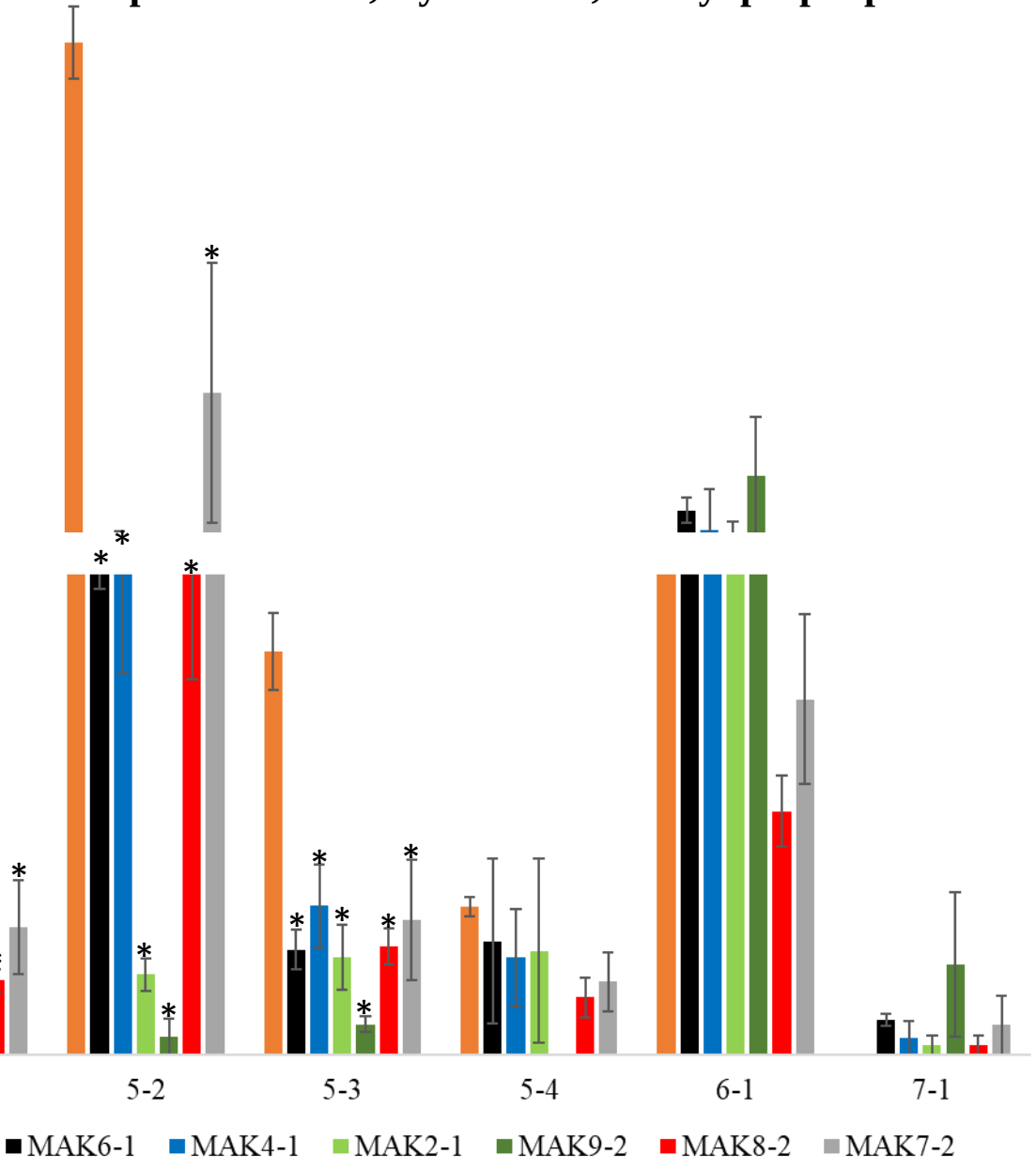

Apocarotenoids, Cyclic ether, Phenyl propanpid PAIP